CHAPTER 3

Drag Force and Drag Coefficient

From: Sadraey M., Aircraft Performance Analysis, VDM Verlag Dr. Müller, 2009

3.1. Introduction

Drag is the enemy of flight and its cost. In chapter 2, major forces that are influencing aircraft motions were briefly introduced. One group of those forces is aerodynamic forces that split into two forces: Lift force or lift, and Drag force or drag. A pre-requisite to aircraft performance analysis is the ability to calculate the aircraft drag at various flight conditions. One of the jobs of a performance engineer is to determine drag force produced by an aircraft at different altitudes, speeds and configurations. This is not an easy task, since; this force is a function of several parameters including aircraft configuration and components. As it was discussed in chapter 2, the drag is a function of aircraft speed, wing area, air density, and its configuration. Each aircraft is designed with a unique configuration, thus, aircraft performance analysis must take into account this configuration. The configuration effect of aircraft drag is represented through the drag coefficient (C_D), plus a reference area that relates to the aircraft.

An aircraft is a complicated three-dimensional vehicle, but for simplicity in calculation, we assume that the drag is a function a two-dimensional area and we call it the reference area. This area could be any area including tail area, wing area and fuselage cross sectional area (i.e., fuselage cross section), fuselage surface area, and even aircraft top-view area. No matter what area is selected, the drag force must be the same. This unique drag comes from the fact that the drag coefficient is a function of the reference area. Therefore, if we select a small reference area, the drag coefficient shall be large, but if we choose a large reference area, the drag coefficient shall be small. In an air vehicle with a small wing area (e.g., high-speed missile), the fuselage cross-sectional area (normal to the flow) is often considered as the reference area. However, in an aircraft with a large wing, the top-view of wing; planform area (in fact gross wing area) is often assumed to be the reference area.

The measurement of this area is easy; and it usually includes the most important aerodynamic part of the aircraft. This simplified reference area is compensated with the complicated drag coefficient, as we discussed in chapter 2.

$$D = \frac{1}{2}\rho V^2 S C_D \tag{3.1}$$

The drag coefficient (C_D) is a non-dimensional parameter, but it takes into account every aerodynamic configuration aspect of the aircraft including large components as wing, tail, fuselage engine, and landing gear; and small elements such as rivets and antenna. This coefficient has two main parts (as will be explained in the next section). The first part is referred to as lift-related drag coefficient or induced drag coefficient (C_{Di}) and the second part is called zero-lift drag coefficient (C_{Do}). The calculation of the first one is not very hard, but it takes a long time and energy to determine the second part. In large transport aircraft, this task is done by a group of engineers up to twenty engineers for a time period of up to six months. For this reason, a large portion of this chapter is devoted to the calculation of C_{Do}. This calculation is not only time consuming, but also is very sensitive, since it influences every aspect of aircraft performance.

One of the occasions in which the drag is considered a beneficial factor and is effectively used is in parachute. A parachute is a device employed to considerably slow the motion of an object/vehicle through an atmosphere (e.g., Earth or Mars) by increasing drag. Parachutes are used with a variety of loads, including people, food, equipment, and space capsules. Drogue chutes are used to sometimes provide horizontal deceleration of a vehicle (e.g., space shuttle after a touchdown). The parachute is utilized by paratroopers to extremely reduce the terminal speed for a safe landing.

One of the primary functions of aerodynamicists and aircraft designers is to reduce this coefficient. Aircraft designers are very sensitive about this coefficient, because any change in the external configuration of aircraft will change this coefficient and finally aircraft direct operating cost. As a performance engineer, you must be able to estimate the C_{Do} of any aircraft just by looking at its three-view with an accuracy of about 30%. As you spend more time for calculation, this estimation will be more accurate, but will never be exact, unless you use an aircraft model in a wind tunnel or flight test measurements with real aircraft model. The method presented in this chapter is about 90% accurate for subsonic aircraft and 85% for supersonic aircraft.

3.2. Drag Classification

Drag force is the summation of all forces that resist against aircraft motion. The calculation of the drag of a complete aircraft is a difficult and challenging task, even for the simplest configurations. We will consider the separate sources of drag that contribute to the total drag of an aircraft. The variation of drag force as a function of airspeed looks like a graph of parabola. This indicates that the drag initially reduces with airspeed, and then increases as the airspeed increases. It demonstrates that there are some parameters that will decrease drag as the velocity increases; and there are some other parameters that will increase drag as the velocity increases. This observation shows us a nice direction for drag classification. Although the drag and the drag coefficient can be expressed in a number of ways, for reasons of simplicity and clarity, the parabolic drag polar will be

used in all main analyses. Different references and textbooks use different terminology, so it may confuse students and engineers. In this section, a list of definitions of various types of drag is presented, and then a classification of all of these drag forces is described.
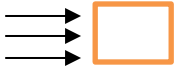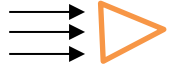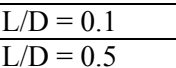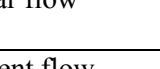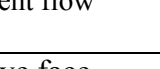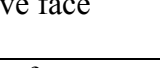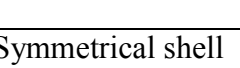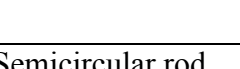
Induced Drag: The drag that results from the generation of a trailing vortex system downstream of a lifting surface with a finite aspect ratio. In another word, this type of drag is induced by the lift force.

Parasite Drag: The total drag of an airplane minus the induced drag. Thus, it is the drag not directly associated with the production of lift. The parasite drag is composed of drag of various aerodynamic components; the definitions of which follow.

Skin Friction Drag: The drag on a body resulting from viscous shearing stresses (i.e., friction) over its contact surface (i.e., skin). The drag of a very streamlined shape such as a thin, flat plate is frequently expressed in terms of a skin friction drag. This drag is a function of Reynolds number. There are mainly two cases where the flow in the boundary layer is entirely laminar or entirely turbulent over the plate. The Reynolds number is based on the total length of the object in the direction of the velocity. In a usual application, the boundary layer is normally laminar near the leading edge of the object undergoing transition to a turbulent layer at some distance back along the surface.

A laminar boundary layer begins to develop at the leading edge and its thickness grows in downstream. At some distance from the leading edge the laminar boundary becomes unstable and is unable to suppress disturbances imposed on it by surface roughness or fluctuations in the free stream. In a distance the boundary layer usually undergoes a transition to a turbulent boundary layer. The layer suddenly increases in thickness and is characterized by a mean velocity profile on which a random fluctuating velocity component is superimposed. The distance, from the leading edge of the object to the transition point can be calculated from the transition Reynolds number. Skin friction factor is independent of surface roughness in laminar flow, but is a strong function of surface roughness in turbulent flow due to boundary layer.
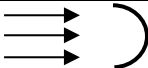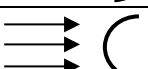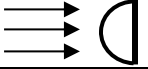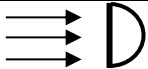
Form Drag (sometimes called **Pressure Drag**): The drag on a body resulting from the integrated effect of the static pressure acting normal to its surface resolved in the drag direction. Unlike the skin friction drag that results from viscous shearing forces tangential to a body's surface, form drag results from the distribution of pressure normal to the body's surface. In an extreme case of a flat plate normal to the flow, the drag is totally the result of an imbalance in the pressure distribution. As with skin friction drag, form drag is generally dependent on Reynolds number. Form drag is based on the projected frontal area. As a body begins to move through the air, the vorticity in the boundary layer is shed from the upper and lower surfaces to form two vortices of opposite rotation. A number of symmetrical shapes having drag values [13] at low speed are illustrated in Table 3.1. The drag coefficient values in this table are based on the frontal area. In this table, the flow is coming from left to the right.

No	Body	Status	Shape		C_D
1	Square rod	Sharp corner			2.2
		Round corner			1.2
2	Circular rod	Laminar flow			1.2
		Turbulent flow			0.3
3	Equilateral triangular rod	Sharp edge face			1.5
		Flat face			2
4	Rectangular rod	Sharp corner		L/D = 0.1	1.9
				L/D = 0.5	2.5
				L/D = 3	1.3
		Round front edge		L/D = 0.5	1.2
				L/D = 1	0.9
				L/D = 4	0.7
5	Elliptical rod	Laminar flow		L/D = 2	0.6
				L/D = 8	0.25
		Turbulent flow		L/D = 2	0.2
				L/D = 8	0.1
6	Symmetrical shell	Concave face			2.3
		Convex face			1.2
7	Semicircular rod	Concave face			1.2
		Flat face			1.7

a. Two dimensional bodies (L: length along flow, D; length perpendicular to the flow)

No	Body	Laminar/turbulent	Status	C_D
1	Cube	Re > 10,000		1.05
2	Thin circular disk	Re > 10,000		1.1
3	Cone ($\theta = 30^\circ$)	Re > 10,000		0.5
4	Sphere	Laminar Re $\leq 2\times10^5$		0.5
		Turbulent Re $\geq 2\times10^6$		0.2
5	Ellipsoid	Laminar Re $\leq 2\times10^5$		0.3-0.5
		Turbulent Re $\geq 2\times10^6$		0.1-0.2
6	Hemisphere	Re > 10,000	Concave face	0.4
		Re > 10,000	Flat face	1.2
7	Rectangular plate	Re > 10,000	Normal to the flow	1.1 - 1.3
8	Vertical cylinder	Re $\leq 2\times10^5$	L/D = 1	0.6
			L/D = ∞	1.2
9	Horizontal cylinder	Re > 10,000	L/D = 0.5	1.1
			L/D = 8	1
10	Parachute	Laminar flow		1.3

b. Three dimensional bodies (L: length, D; diameter)

Table 3.1. Drag coefficient values for various geometries and shapes

Interference Drag: The increment in drag resulting from bringing two bodies in proximity to each other. For example, the total drag of a wing-fuselage combination will usually be greater than the sum of the wing drag and fuselage drag independent of each other.

Trim Drag: The increment in drag resulting from the (tail) aerodynamic forces required to trim the aircraft about its center of gravity. Trim drag usually is a form of induced and form drag on the horizontal tail.

Profile Drag: Usually taken to mean the total of the skin friction drag and form drag for a two-dimensional airfoil section.

Cooling Drag: The drag resulting from the momentum lost by the air that passes through the power plant installation for the purpose of cooling the engine.

Wave Drag: This drag; limited to supersonic flow; is a form of induced drag resulting from non-canceling static pressure components to either side of a shock wave acting on the surface of the body from which the wave is emanating.
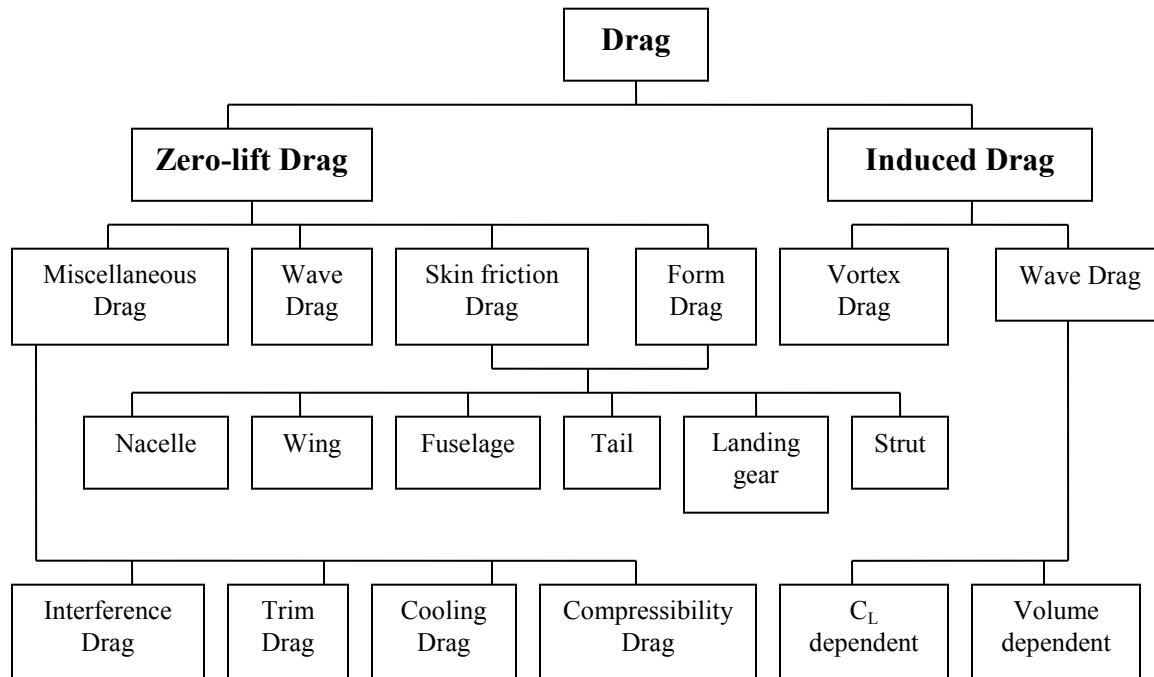
Figure 3.1. *Drag classification*

The material to follow will consider these various types of drag in detail and will present methods of reasonably estimating their magnitudes. Figure 3.1 illustrates the drag classification into two major groups.

For a conventional aircraft, the drag is divided into two main parts; lift related drag, and non-lift related drag. The first part is called induced drag (D_i), because this drag is induced by lift (pressure). The second part is referred to as zero-lift drag (D_o), since it does not have any influence from lift, and is mainly originates from shear stress.

$$D = D_o + D_i \qquad (3.2)$$

a. **Induced drag:** The induced drag is the drag directly associated with the production of lift. This results from the dependency of the induced drag on the angle of attack. As the angle of attack of the aircraft (i.e., lift coefficient) varies, this type of drag is changed. The induced drag in itself consists of two parts. The first part originates from vortices around wing, tail, fuselage, and other components. The second part is because of air compressibility effect. In low subsonic flight, it is negligible, but is high subsonic and transonic flight, must be taken into account. In supersonic flight, wave drag (D_w) is added to the induced drag. The reason is to account for the contribution of shock wave. The wing is the major aircraft component contributor for the lift production. Thus, about 80% of the induced drag comes from wing; about 10% comes from tail; and the rest originate from other components. The induced drag is a function of airspeed, air density, reference area, and the lift coefficient:

$$D_i = \frac{1}{2}\rho V^2 S C_{D_i} \qquad (3.3)$$

In this equation, the coefficient C_{Di} is called induced drag coefficient. The method to calculate this coefficient will be introduced in the next section. Figure 3.2 shows the behavior of induced drag as a function of airspeed. As the airspeed increases, the induced drag decreases; so the induced drag is inversely a function of airspeed.
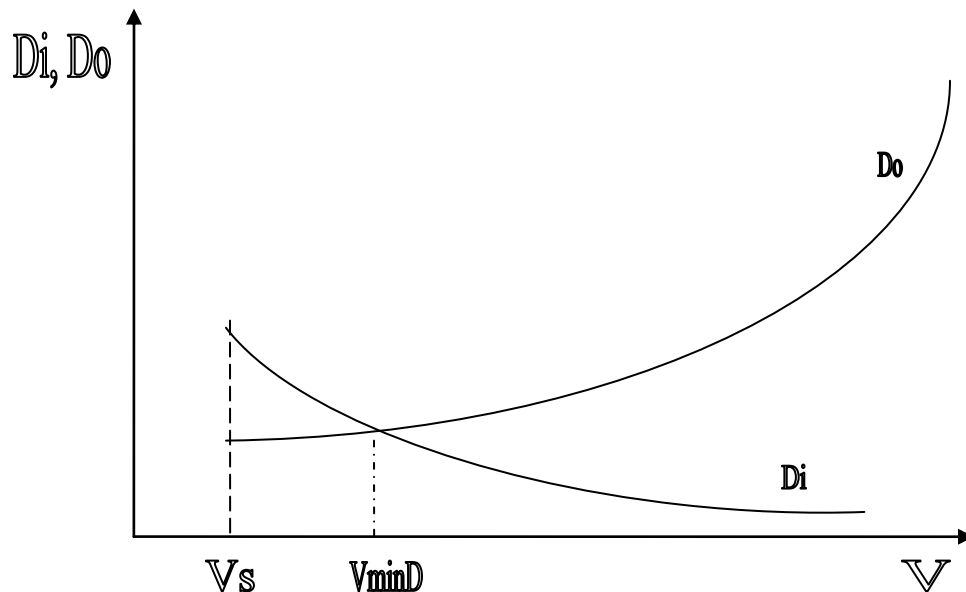

Figure 3.2. *Variations of D_o and D_i versus velocity*

b. **Zero-lift drag:** The zero-lift drag includes all types of drag that do not depend on production of the lift. Every aerodynamic component of aircraft (i.e. the

components that are in direct contact with flow) generates zero-lift drag. Typical components are wing, horizontal tail, vertical tail, fuselage, landing gear, antenna, engine nacelle, and strut. The zero-lift drag is a function of airspeed, air density, reference area, and the external shape of the components:

$$D_o = \frac{1}{2}\rho V^2 S C_{Do} \tag{3.4}$$

In this equation, the coefficient C_{Do} is called *zero-lift drag coefficient*. The method to calculate this coefficient will be introduced in Section 3.4. Figure 3.2 shows the variation of zero-lift drag as a function of airspeed. As the airspeed increases, the induced increases too; so the zero-lift drag is directly a function of airspeed.

From the equations 3.1, 3.2, 3.3 and 3.4; one can conclude that drag coefficient has two components:

$$C_D = C_{Do} + C_{Di} \tag{3.5}$$

The calculation of C_{Di} is not a big deal and will be explained in the next section; but the calculation of C_{Do} is very challenging, tedious, and difficult. Major portion of this chapter is devoted to calculation of C_{Do}. In fact, the main idea behind this chapter is about calculation of C_{Do}.

3.3. Drag Polar

The aircraft drag may be mathematically modeled by variety of methods. It seems natural to seek the similarity of variation of drag due to a flight parameter to a standard figure or geometry. We are looking for an accurate, but simple mathematical model, and a math expression for such curves as in figure 3.3.

As figure 3.3 and equation 3.5 show, the drag is composed of two terms, one proportional to the square of airspeed (i.e., V^2) and the other one inversely proportional to V^2. The first term, called zero-lift drag represents the aerodynamic cleanness with respect to frictional characteristics, and shape and protuberances such as cockpit, antennae, or external fuel tanks. It increases with the aircraft velocity and is the main factor in determining the aircraft maximum speed. The second term represents induced drag (drag due to the lift). Its contribution is highest at low velocities, and it decreases with increasing flight velocities. If we combine (indeed add) these two curves (D_i and D_o) in Figure 3.2, we will have a parabolic curve such as what shown in figure 3.3. The parabolic drag model is not exact; but accurate enough for the purpose of performance calculation. A similar behavior is observed for the variation of drag coefficient versus lift coefficient. Drag polar is a math model for the variation of drag coefficient as a function of lift coefficient.
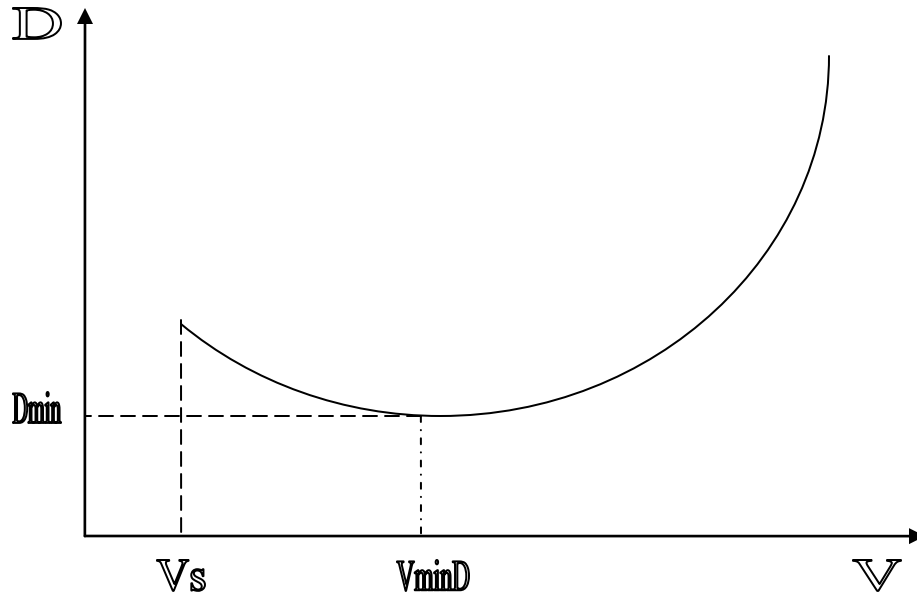
Figure 3.3. *Variations of drag versus airspeed*

Although the drag and the drag coefficient can be expressed in a number of ways, for reasons of simplicity and clarity, the parabolic drag polar will has been selected in the analysis. This is true only for subsonic flight. For the existing supersonic aircraft, the drag cannot be adequately described by such a simplified expression. Exact calculations must be carried out using extended equations or tabular data. However, the inclusion of more precise expressions for drag at this stage will not greatly enhance basic understanding of performance, and thus, will be included only in some calculated examples and exercises. Note that the curve begins from stall speed, since an aircraft is not able to maintain a sustained level flight at any speed below the stall speed. The same conclusion is true for the variation of drag coefficient (C_D) versus lift coefficient (C_L) as shown in figure 3.4.

A non-dimensionalized form of figure 3.3; the variation of drag coefficient versus lift coefficient; is demonstrated in figure 3.4. It can be proved that a second order parabolic curve can mathematically describe such a curve with an acceptable accuracy:

$$y = a + bx^2 \tag{3.6}$$

where y may be replaced with C_D and x may be replaced with C_L. Therefore, drag coefficient versus lift coefficient is modeled with the following parabolic model:

$$C_D = a + bC_L^{\,2} \tag{3.7}$$

Now, we need to determine the values or expressions for "a" and "b" in this equation. In a symmetrical parabolic curve, the parameter "a" is the minimum value for parameter "y". hence, in a parabolic curve of C_D versus C_L, the parameter "a" must be the minimum amount of drag coefficient (C_{Dmin}). We refer this minimum value of drag

coefficient as C_{Do} as it means the value of C_D when the lift is zero. The corresponding value for "b" in equation 3.7 must be found through experiment. Aerodynamicists have represented this parameter with the symbol of "K", and refer to it as induced drag correction factor. The induced drag correction factor is inversely proportional to the wing aspect ratio (AR) and wing Oswald efficiency factor (e). The mathematical relationship is as follows:
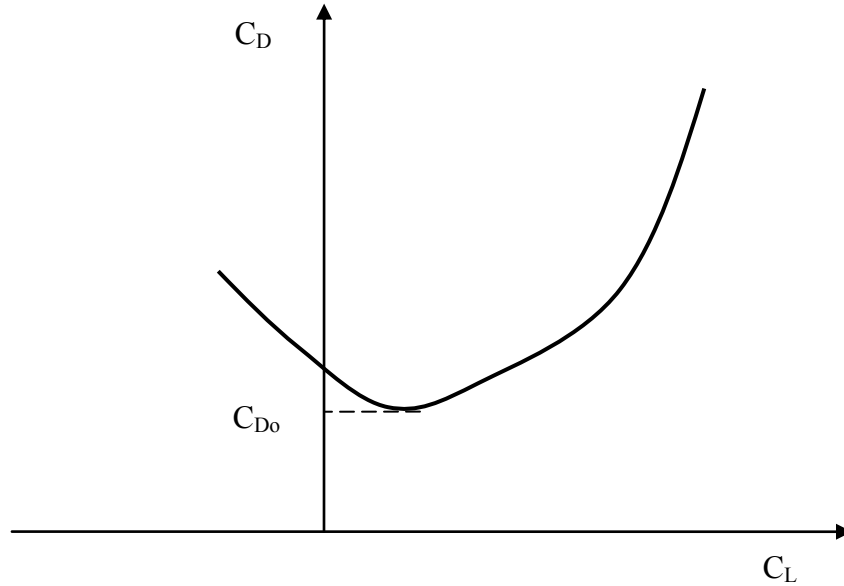
Figure 3.4. *A typical variations of C_D versus C_L*

$$K = \frac{1}{\pi \cdot e \cdot AR} \tag{3.8}$$

The wing aspect ratio is the ratio between the wing span (b) and the mean aerodynamic chord (MAC or C). The ratio can be reformatted to be a function of the wing area (S) and wing span as follows:

$$AR = \frac{b}{C} = \frac{bb}{Cb} = \frac{b^2}{S} \tag{3.9}$$

The wing Oswald efficiency factor represents the efficiency of a wing in producing lift, and is a function of wing aspect ratio and the leading edge sweep angle, Λ_{LE}. If the lift distribution is parabolic, the Oswald efficiency factor is assumed to be the highest (i.e., 100% or 1). The Oswald efficiency factor is usually between 0.7 and 0.9. Ref. 9 introduces the following two expressions for estimation of Oswald efficiency factor:

$$e = 4.61\left(1 - 0.045 AR^{0.68}\right)\left[\cos(\Lambda_{LE})\right]^{0.15} - 3.1 \tag{3.10a}$$
$$e = 1.78\left(1 - 0.045 AR^{0.68}\right) - 0.64 \tag{3.10b}$$

Equation 3.10a is for swept wings with leading edge sweep angles of more than 30 degrees and equation 3.10b is for rectangular wings (without sweep). These two formulas are only valid for wing with high aspect ratio (e.g., AR more than 6).
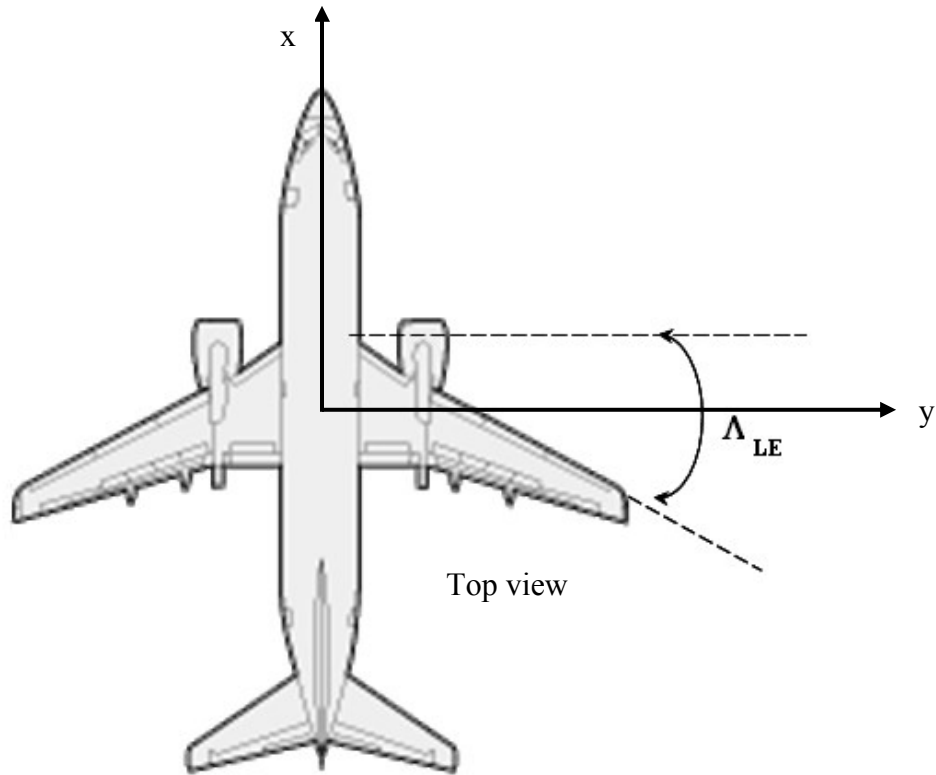
Figure 3.5. *Wing leading edge sweep angle*

The wing leading edge sweep angle (see figure 3.5) is the angle between wing leading edge and the aircraft y-axis. Table 3.2 shows wing Oswald efficiency factor for several aircraft. The value of "e" is decreased at high angle of attacks (i.e., low speed) up to about 30%.

Figure 3.6. *The glider Schleicher ASW22 with wing span of 25 meter and C_{Do} of 0.016*

Employing the induced drag correction factor (K), we have a mathematical expression for the variation of drag coefficient versus lift coefficient.

$$C_D = C_{D_o} + KC_L{}^2 \tag{3.11}$$

This equation is sometimes referred to as aircraft "*drag polar*". The main challenge in this equation is the calculation of zero-lift drag coefficient. Table 3.2 shows typical values of C_{Do} for several aircraft. The values in this table are the lowest values; which means at the lowest airspeed (usually low subsonic speeds). Gliders or sailplanes are aerodynamically the most efficient aircraft (with C_{Do} as low as 0.01) and agricultural aircraft are aerodynamically the least efficient aircraft (with C_{Do} as high as 0.08) .The lift coefficient is readily found from equation 2.3. Compare the glider Schleicher ASW22 that has a C_{Do} of 0.016 (Figure 3.6) with the agricultural aircraft Dromader, PZL M-18 that has a C_{Do} of 0.058 (figure 3.7).

Figure 3.7. *Agricultural aircraft Dromader, PZL M-18 with C_{Do} of 0.058*

Comparison between equations 3.5 and 3.11 yields the following relationship.

$$C_{D_i} = KC_L{}^2 \tag{3.12}$$

So, induced drag is proportional to the square of lift coefficient. Figure 3.4 shows the effect of lift coefficient (induced drag) on drag coefficient.

3.4. Calculation of C_{Do}

The equation 3.11 implies that the calculation of aerodynamic force of drag is dependent on zero-lift drag coefficient (C_{Do}). Since the performance analysis is based on aircraft drag, the accuracy of aircraft performance analysis relies heavily on the calculation accuracy of C_{Do}. This section is devoted to the calculation of zero-lift drag coefficient and is the most important section of this chapter. The method by which the zero-lift drag coefficient is determined is called "*build-up*" technique.

No	Aircraft type	C_{Do}	e
1	Twin-engine piton prop	0.022-0.028	0.75-0.8
2	Large turboprop	0.018-0.024	0.8-0.85
3	Small GA with retractable landing gear	0.02-0.03	0.75-0.8
4	Small GA with fixed landing gear[1]	0.025-0.04	0.65-0.8
5	Agricultural aircraft with crop duster	0.07-0.08	0.65-0.7
6	Agricultural aircraft without crop duster	0.06-0.065	0.65-0.75
7	Subsonic jet	0.014-0.02	0.75-0.85
8	Supersonic jet	0.02-0.04	0.6-0.8
9	Glider	0.012-0.015	0.8-0.9
10	Remote controlled model aircraft	0.025-0.045	0.75-0.85

Table 3.2. *Typical values of "C_{Do}" and "e" for several aircraft*

As figure 3.8 illustrates, external aerodynamic components of an aircraft are all contributing to aircraft drag. Although only wing; and to some extents, tail; have aerodynamic function (i.e., to produce lift), but every component (either large size such as the wing or small size such as a rivet) that has direct contact with air flow, is doing some types of aerodynamic functions (i.e., producing drag). Thus, in order to calculate zero-lift drag coefficient of an aircraft, we must include every contributing item. The C_{Do} of an aircraft is simply the summation of C_{Do} of all contributing components.
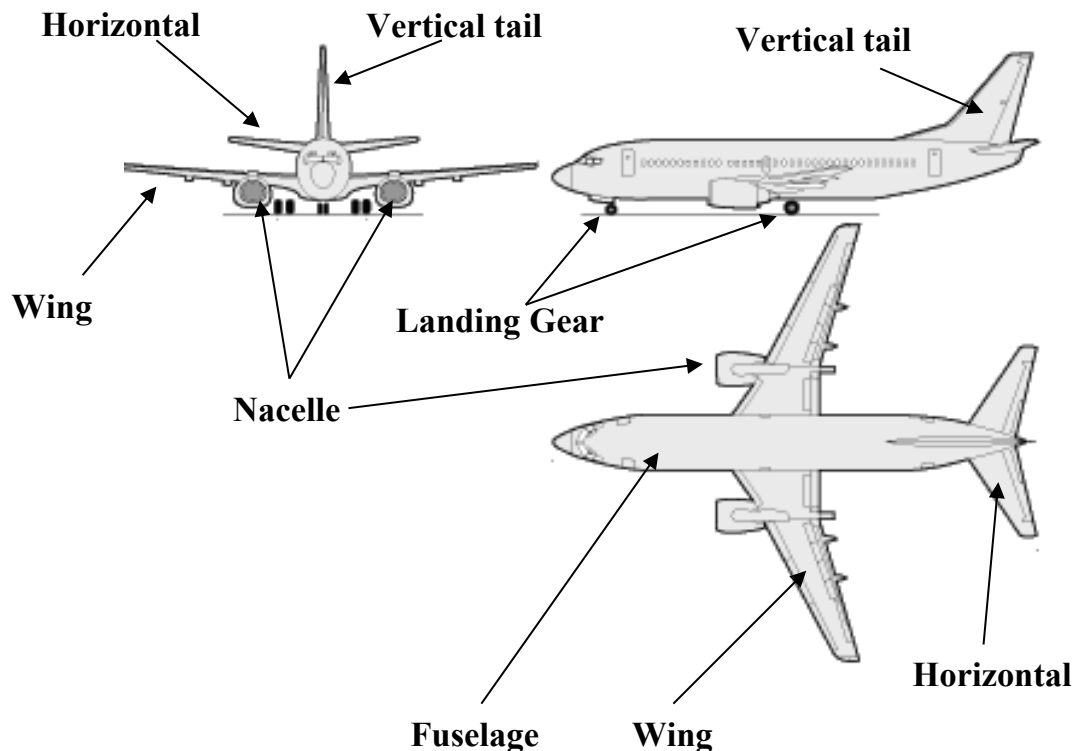

Figure 3.8. *Major components of Boeing 737 contributing to C_{Do}*

---

[1] This also refers to a small GA with retractable landing gear during take-off

$$C_{D_o} = C_{D_{o_f}} + C_{D_{o_w}} + C_{D_{o_{ht}}} + C_{D_{o_{vt}}} + C_{D_{o_{LG}}} + C_{D_{o_N}} + C_{D_{o_S}} + C_{D_{o_{HLD}}} + \dots \tag{3.13}$$

where C_{Dof}, C_{Dow}, C_{Doht}, C_{Dovt}, C_{DoLG}, C_{DoN}, C_{DoS}, C_{DoHLD}, are respectively representing fuselage, wing, horizontal tail, vertical tail, landing gear, nacelle, strut, high lift device (such as flap) contributions in aircraft C_{Do}. The three dots at the end of equation 3.13 illustrates that there are other components that are not shown here. They include non-significant components such as antenna, pitot tube, stall horn, wires, interference, and wiper.

Every component has a positive contribution, and no component has negative component. In majority of conventional aircraft, wing and fuselage are each contributing about 30%-40% (totally 60%-80%) to aircraft C_{Do}. All other components are contributing about 20%-40% to C_{Do} of an aircraft. In some aircraft (e.g., hang gliders), there is no fuselage, so it does not have any contribution in C_{Do}; instead the human pilot plays a similar role to fuselage.

In each subsection of this section, a technique is introduced to calculate the contribution of each component to C_{Do} of an aircraft. The primary reference for these techniques and equations is Reference 1. Majority of the equations are based on flight test data and wind tunnel test experiments, so the build-up technique is relying mainly on empirical formulas.

3.4.1. Fuselage

The zero-lift drag coefficient of a fuselage is given by the following equation:

$$C_{D_{o_f}} = C_f f_{LD} f_M \frac{S_{wet_f}}{S} \tag{3.14}$$

where, C_f is skin friction coefficient, and is a non-dimensional number. It is determined based on the Prandtl relationship as follows:

$$C_f = \frac{0.455}{\left[\log_{10}(\mathrm{Re})\right]^{2.58}} \qquad \text{(Turbulent flow) (3.15a)}$$

$$C_f = \frac{1.327}{\sqrt{\mathrm{Re}}} \qquad \text{(Laminar flow) (3.15b)}$$

The parameter Re is called *Reynolds number* and has a non-dimensional value. It is defined as:

$$\mathrm{Re} = \frac{\rho V L}{\mu} \tag{3.16}$$

where ρ is the air density, V is aircraft true airspeed, μ is air viscosity, and L is the length of the component in the direction of flight. For a fuselage, L is the fuselage length. For lifting surfaces such as wing and tail, L is the mean aerodynamic chord.

Equation 3.15a is for a purely turbulent flow and equation 3.15b is for a purely laminar flow. Most aircraft are frequently experiencing a combination of laminar and turbulent flow over fuselage and other component. There are aerodynamic references (e.g., [8] and [10]) that recommend technique to evaluate the ratio between laminar and turbulent flow over any aerodynamic component. The transition point from laminar to turbulent flow may be evaluated by these references. For simplicity, they are not reproduced here. Instead, you are recommended to assume that the flow is either completely laminar or completely turbulent. The assumption of complete turbulent flow provides a better result; since over-estimation of drag is much better than its under-estimation.

In theory, the flow is laminar when Reynolds number is below 4,000. However, in practice, turbulence is not effective when Reynolds number is below 200,000; so when the Reynolds number is less than 200,000, you may assume laminar flow. In addition, when the Reynolds number is higher than 2,000,000, you may assume turbulent flow. As a rule of thumb, in low subsonic flight, the flow is mostly laminar, but in high subsonic and transonic speed, it becomes mostly turbulent. Supersonic and hypersonic flight experiences a complete turbulent flow over every component of aircraft. A typical current aircraft may have laminar flow over 10%-20% of the wing, fuselage and tail. A modern aircraft such as the Piaggio 180 can have laminar flow over as much as 50% of the wing and tails, and about 40%-50% of the fuselage.

The second parameter in equation 3.14 (f_{LD}) is a function of fuselage length-to-diameter ratio. It is defined as:

$$f_{LD} = 1 + \frac{60}{(L/D)^3} + 0.0025\left(\frac{L}{D}\right) \tag{3.17}$$

where L is the fuselage length and D is its maximum diameter. If the cross section of the fuselage is not a circle, you need to find its equivalent diameter. The third parameter in equation 3.14 (f_M) is a function of Mach number (M). It is defined as

$$f_M = 1 - 0.08M^{1.45} \tag{3.18}$$

The last two parameters in equation 3.14 are S_{wetf} and S, they are the wetted area of the fuselage and the wing reference area respectively.

Wetted area is the actual surface area of the material making up the skin of the airplane - it is the total surface area that is in actual contact with, i.e., wetted by, the air in which the body is immersed. Indeed, the wetted surface area is the surface on which the pressure and shear stress distributions are acting; hence it is a meaningful geometric

quantity when one is discussing aerodynamic force. However, the wetted surface area is not easily calculated, especially for complex body shapes.
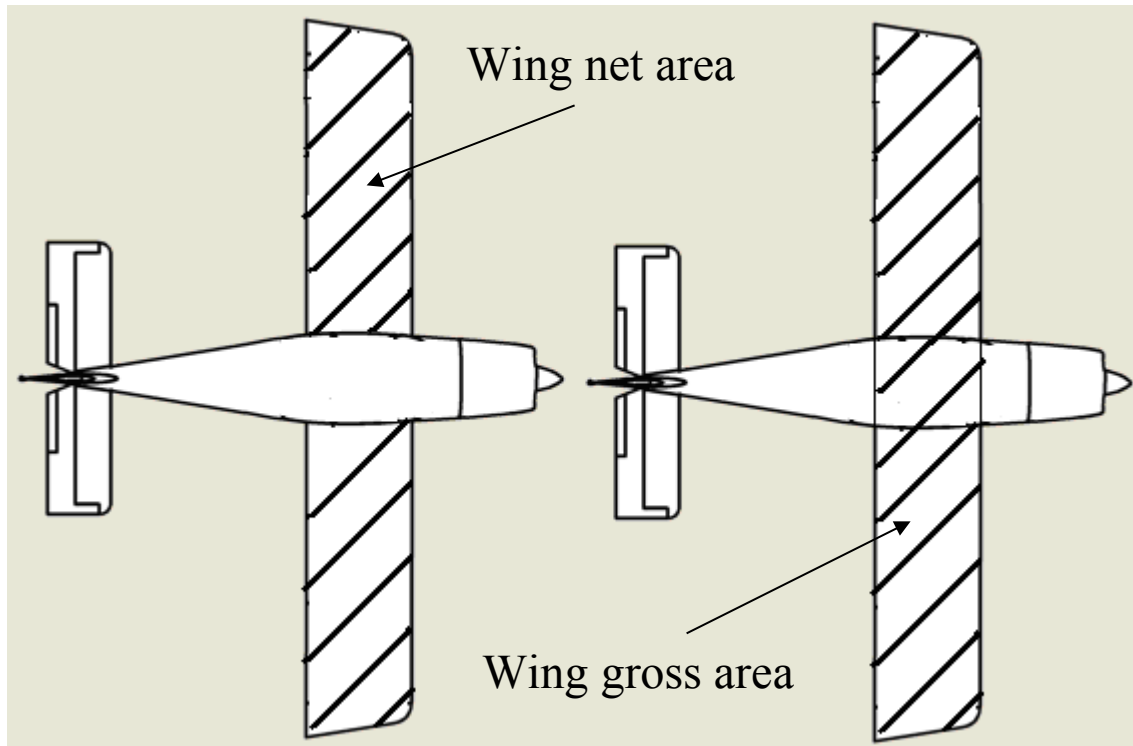
Figure 3.9. *Wing gross area and wing net (exposed) area*

A comment seems necessary regarding the reference area, S in equation 3.14. The parameter S is nothing other than just a reference area, suitably chosen for the definition of the force and moment coefficients.

The reference area (S) is simply an area as a basis or reference that can be arbitrarily specified. This selection is primarily done for the convenience. The reference area (S) for a conventional aircraft is the projected area that we see when we look down on the wing from top view, including the fuselage section between two parts of the wing. For this reason, for wings as well as entire airplanes, the wing planform area is usually used as S in the definitions of C_L, C_D, and C_m. However, if we are considering the lift and drag of a cone, or some other slender, missile like body, then the reference area, S is frequently taken as the base area of the cone or fuselage. Figure 3.9 highlights the difference between wing net area and wing gross area. Thus, when we say wing planform area, we mean wing gross area. The reference area selection assumption will not incur any error in the calculation of wing drag and aircraft drag. The reason is that the drag coefficient will be automatically adjusted by this selection.

Whether we take the planform area, base area, or any other areas to a given body shape for S, it is still a measure of the relative size of different bodies which are geometrically similar. As long as you are consistent, you may take any significant area as the reference area. What is important in the calculation of C_L, C_D, and C_m is to divide the

aerodynamic force/moment to a noticeable area. It is urged to an aircraft performance engineer that whenever you take a data for C_L, C_D, or C_m from the technical literature, make certain that you know what geometric reference area was used for S in the calculation. Then use that same area when making calculations involving lift, drag and pitching moment. Otherwise, the results will involve significant inaccuracies. In contrast with S_{wet}, it is much easier to calculate the planform area of a wing.

3.4.2. Wing, Horizontal Tail, and Vertical Tail

Since wing, horizontal tail and vertical tail are three lifting surfaces, they are treated in a similar manner. The zero-lift drag coefficient of the wing ($C_{D_{o_w}}$), horizontal tail ($C_{D_{o_{ht}}}$), and vertical tail ($C_{D_{o_{vt}}}$), are respectively given by the following equations:

$$C_{D_{o_w}} = C_{f_w} f_{tc_w} f_M \left(\frac{S_{wet_w}}{S} \right) \left(\frac{C_{d_{\min w}}}{0.004} \right)^{0.4} \tag{3.19}$$

$$C_{D_{o_{ht}}} = C_{f_{ht}} f_{tc_{ht}} f_M \left(\frac{S_{wet_{ht}}}{S} \right) \left(\frac{C_{d_{\min ht}}}{0.004} \right)^{0.4} \tag{3.20}$$

$$C_{D_{o_{vt}}} = C_{f_{vt}} f_{tc_{vt}} f_M \left(\frac{S_{wet_{vt}}}{S} \right) \left(\frac{C_{d_{\min vt}}}{0.004} \right)^{0.4} \tag{3.21}$$

In these equations, C_{fw}, C_{fht}, C_{fvt} are similar to what we defined for fuselage in formula 3.15. The only difference is that the equivalent value of L in Reynolds number (equation 3.22) for wing, horizontal tail, and vertical tail are their mean aerodynamic chords (MAC or $\overline{C}$). In another word, the definition of Reynolds number for a lifting surface (e.g., wing) is:

$$\mathrm{Re} = \frac{\rho V \overline{C}}{\mu} \tag{3.22}$$

where the mean aerodynamic chord is calculated by

$$\overline{C} = \frac{2}{3} C_r \left[1 + \lambda - \frac{\lambda}{1+\lambda} \right] \tag{3.23}$$

where C_r denotes root chord (See figure 3.10), and λ is the taper ratio; the ratio between tip chord (C_t) and root chord (C_r):

$$\lambda = \frac{C_t}{C_r} \tag{3.24}$$

The parameter f_{tc} is a function of thickness ratio and is given by

$$f_{tc} = 1 + 2.7 \left(\frac{t}{c} \right)_{\max} + 100 \left(\frac{t}{c} \right)_{\max}^4 \tag{3.25}$$

where $\left(\dfrac{t}{c}\right)_{max}$ is the maximum thickness-to-chord ratio of the wing, or the tail. Generally speaking, the maximum thickness to chord ratio for a wing is about 12% to18%, and for a tail is about 9% to 12%. The parameter S_{wet} in equation 3.12 is the wing or tail wetted area.

The parameters $Swet_w$, $Swet_{ht}$, and $Swet_{vt}$ denote wetted area of the wing, horizontal tail, and vertical tail respectively. Unlike reference area, the wetted area is based on the exposed area, and not the gross area. Due to of the special curvature of the wing and tail airfoil sections, it may seem time consuming to calculate the accurate wetted area of a wing or a tail. There is a simplified method to determine the wetted area of a lifting surface with an acceptable accuracy. Since the wing and tail are not too thick (average about 15%), it may be initially assumed that, the wetted area is about twice that of the net or exposed area (see figure 3.9). To be more accurate, you may assume the lifting as a thing box with average thickness equal to half of the airfoil thickness. According to this assumption, the wetted area is given as:
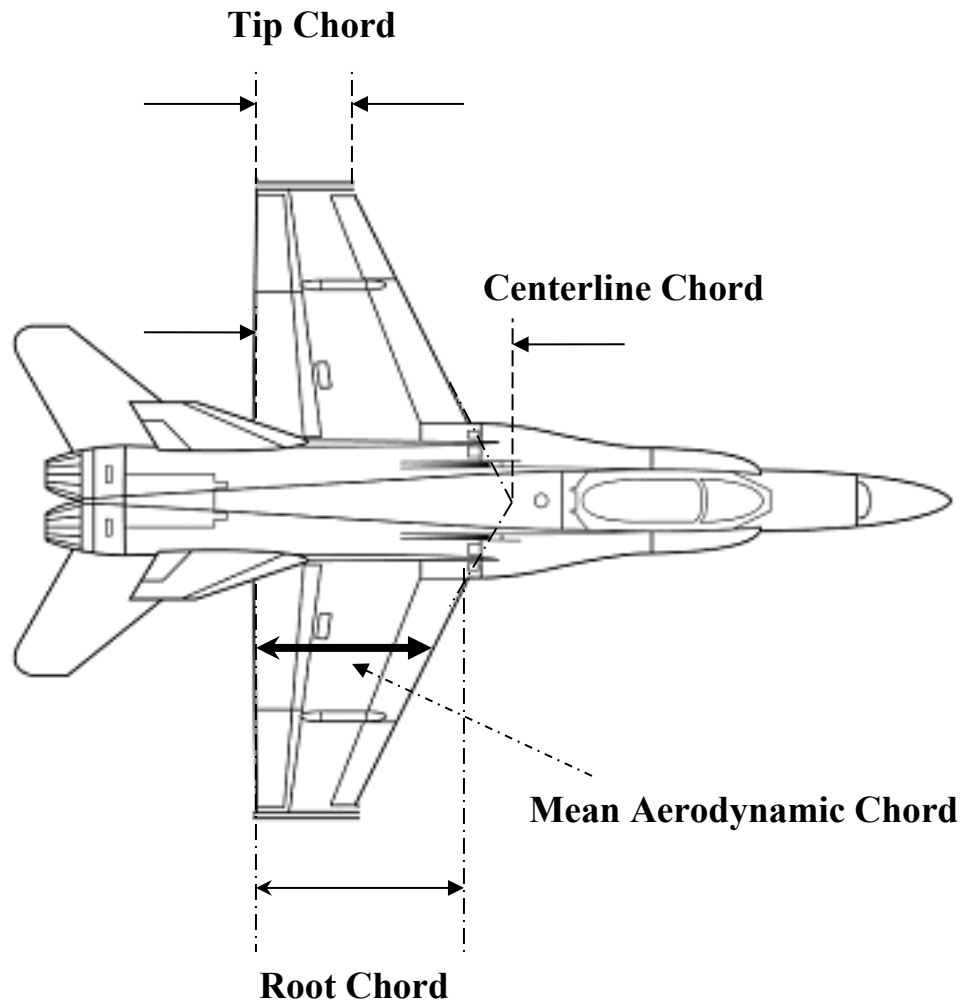
Tip Chord

Centerline Chord

Mean Aerodynamic Chord

Root Chord

Figure 3.10. *Wing Mean Aerodynamic Chord (MAC)*

$$S_{wet} = 2\left[1 + 0.5\left(\frac{t}{c}\right)_{max}\right]bC \tag{3.26}$$

For ultimate accuracy, you need to employ a CAD software package (e.g., AutoCad or SolidWorks) to calculate it with a high accuracy.

The parameter C_{dmin} in equations 3.19, 3.20, and 3.21 is the minimum drag coefficient of the airfoil cross section of the wing or tail. It can be readily extracted from a C_d-C_l curve of the airfoil. One example is illustrated in figure 3.11 for a six series NACA airfoil 63_1-412. Reference [3] is a rich collection of information for a variety of NACA 4 digits, 5 digits, and 6-serieis airfoils. For instance, the NACA airfoil 63_1-412 has a minimum drag coefficient of 0.0048 9 for the clean or flap-up configuration.

Example 3.1
Consider a cargo aircraft with the following features:

$$m = 380,000 \text{ kg} \quad S = 567 \text{ m}^2, \quad MAC = 9.3 \text{ m}, \quad (t/c)_{max} = 18\%, \quad C_{dmin} = 0.0052$$

This aircraft is cruising at sea level with an airspeed of 400 knot. Assume the aircraft C_{Do} is three times the wing C_{Do} (i.e., C_{Dow}), determine the aircraft C_{Do}.

Solution:

$$Re = \frac{\rho V \overline{C}}{\mu} = \frac{1.225 \times (400 \times 0.5144) \times 9.3}{1.785 \times 10^{-5}} = 131,334,640 = 1.31 \times 10^8 \tag{3.16}$$

$$M = \frac{V}{a} = \frac{400 \times 0.5144}{340} = 0.605 \tag{1.20}$$

Due to the high Reynolds number, the air flow over the wing is turbulent, so

$$C_f = \frac{0.455}{[\log_{10}(Re)]^{2.58}} = \frac{0.455}{[\log_{10}(131,334,640)]^{2.58}} = 0.00205 \tag{3.15a}$$

$$f_M = 1 - 0.08 M^{1.45} = 1 - 0.08 \times (0.606)^{1.45} = 0.9614 \tag{3.18}$$

$$f_{tc} = 1 + 2.7\left(\frac{t}{c}\right)_{max} + 100\left(\frac{t}{c}\right)_{max}^4 = 1 + 2.7(0.18) + 100(0.18)^4 = 1.591 \tag{3.25}$$

$$S_{wet} = 2\left[1 + 0.5\left(\frac{t}{c}\right)_{max}\right]bC = 2[1 + 0.5 \times 0.18] \times 567 = 1,236 \ m^2 \tag{3.26}$$

$$C_{D_{ow}} = C_{f_w} f_{tc_w} f_M \left(\frac{S_{wet_w}}{S}\right)\left(\frac{C_{d_{min_w}}}{0.004}\right)^{0.4} \tag{3.19}$$

$$C_{D_{o_w}} = 0.00205 \times 1.591 \times 0.9614 \times \frac{1236}{576} \times \left(\frac{0.0052}{0.004}\right)^{0.4} = 0.0759$$

Therefore the aircraft zero-lift drag coefficient is:

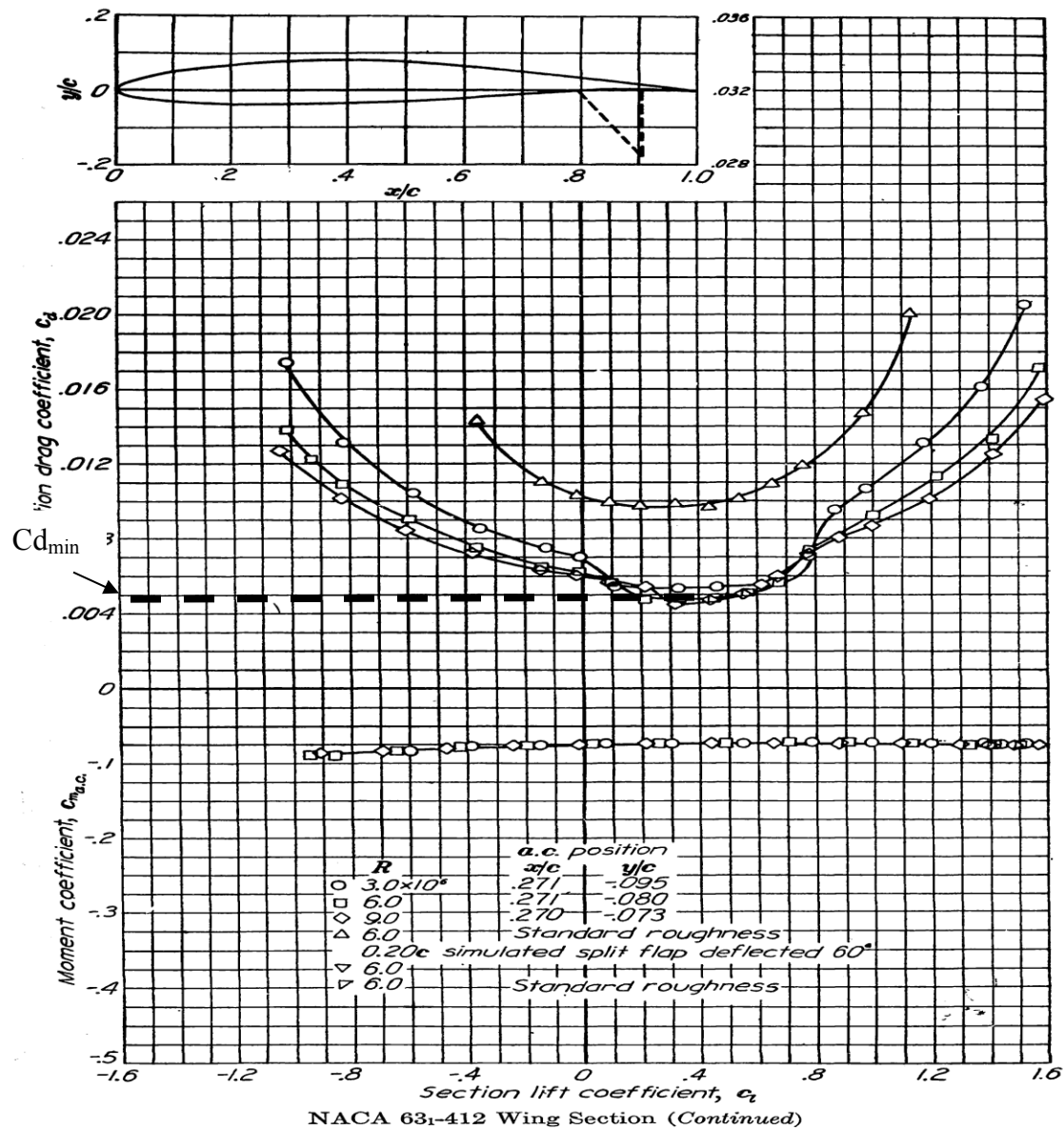$$C_{D_o} = 2.3 C_{D_{o_w}} = 3 \times 0.0759 = 0.0228$$

Figure 3.11. The variations of lift coefficient versus drag coefficient for airfoil NACA 63_1-412 (Ref. 3)

3.4.3. High Lift Devices (HLD)

High lift devices are parts of the wing to increases lift when employed (i.e., deflected). They are usually employed during take-off and landing. Two main groups of high lift devices are leading edge high lift devices (often called flap) and trailing edge high lift devices (e.g., slat). There are many types of wing trailing edge flaps such as split flap, plain flap, single-slotted flap, fowler flap, double-slotted flap, and triple-slotted flap. They are deflected down to increase the camber of the wing, in order to increase lift, so the maximum lift coefficient, C_{Lmax} will be increased. The most effective method used on large transport aircraft is the leading edge slat. A variant on the leading edge slat is a variable camber slotted Kruger flap used on the Boeing 747. The main effect of the wing trailing edge flap is to increase the effective angle of attack of the wing without actually pitching the airplane. The application of high lift devices has a few negative side-effects including an increase in aircraft drag (as will be included in C_{Do}).

3.4.3.1. Trailing Edge High Lift Device

The increase in C_{Do} due to application of trailing edge high lift device (flap) is given by the following empirical formula:

$$C_{D_{o\,flap}} = \left(\frac{C_f}{C}\right) A \cdot (\delta_f)^B \tag{3.27}$$

where C_f/C is the ratio between average flap chord to average wing chord (see figure 3.12) at the flap location and is usually about 0.2. In case where the flap is extended, as in the case for a slotted flap, the C_f represents the extended chord. Furthermore, when a flap is extended, the wing chord (C) is also locally increased. The equation 3.27 is based on a flap with a flap-span-to-wing-span ratio of 70%. In the case where the flap span is different, the results should be revised accordingly.
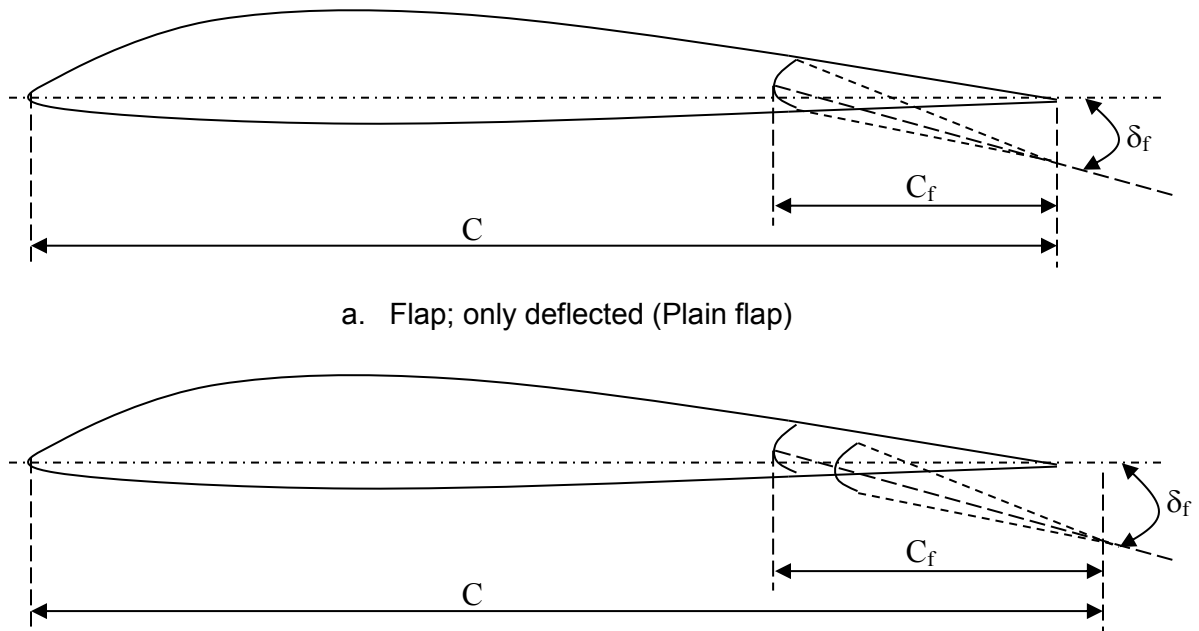
a. Flap; only deflected (Plain flap)

b. Flap; extended while deflected (Slotted flap)

Figure 3.12. *Wing section at the flap location*

Do not confuse this C_f with skin friction coefficient which shares the same symbol. The parameters "A" and "B" are given in the Table 3.3 based on the type of flap. The δ_f is the flap deflection in degrees (usually less than 50 degrees).

No	Flap type	A	B
1	Split flap	0.0014	1.5
2	Plain flap	0.0016	1.5
3	Single-slotted flap	0.00018	2
4	Double-slotted flap	0.0011	1
5	Fowler	0.00015	1.5

Table 3.3. *The values of A and B for different types of flaps*

3.4.3.1. Leading Edge High Lift Device

The increase in C_{Do} due to application of a leading edge high lift device (e.g., slot, and slat) is given by the following empirical formula:

$$C_{D_{o_{sl}}} = \left(\frac{C_{sl}}{C}\right) C_{D_{o_w}}$$

(3.28)

where C_{sl}/C is the ratio between average extended slat chord to average extended wing chord. The C_{Dow} is the wing zero-lift drag coefficient without extending a high lift device (including slat).

3.4.4. Landing Gear

The landing gear (or undercarriage) is the structure (usually struts and wheels) that supports the aircraft weight and facilitates its motion along the surface of the runway when the aircraft is not airborne. Landing gear usually includes wheels and is equipped with shock absorbers for solid ground, but some aircraft are equipped with skis for snow or floats for water, and/or skids. To decrease drag in flight, some landing gears are retracted into the wings and/or fuselage with wheels or concealed behind doors; this is called retractable gear. In the case of retracted landing gear, the aircraft clean C_{Do} is not affected by the landing gear.

When landing gear is fixed (not retracted) in place, it produces an extra drag for the aircraft. It is sometimes responsible for an increase in the aircraft drag as high as 50%. In some aircraft, a fairing is used to decrease the drag of a non-retracted gear (see figure 3.14b). The fairing is a partial cover that has a streamlined shape such as airfoil. The increase in C_{Do} due to wheel of the landing gear is given by the following empirical equation:

$$C_{D_{o_{lg}}} = \sum_{i=1}^{n} C_{D_{lg}} \left(\frac{S_{lg_i}}{S}\right)$$

(3.29)

where S_{lg} is the frontal area of each wheel, and S is the wing reference area. The parameter C_{Dlg} is the drag coefficient of each wheel; that is 0.15, when it has fairing; and is 0.30 when it does not have any fairing (see figure 3.13). The frontal area of each wheel is simply the diameter (d_g) times the width (w_g).

$$S_{lg} = d_g w_g \tag{3.30}$$

a. Without fairing

b. With fairing
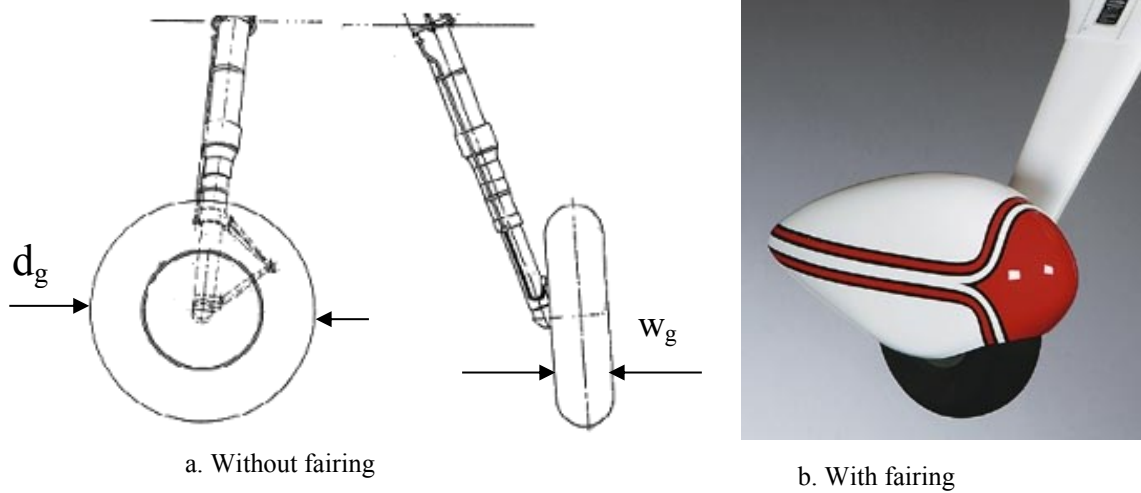
Figure 3.13. *Landing gear and its fairing*

As it is observed in equation 3.29, every wheel that is experiencing air flow must be accounted for drag. For this reason, subscript "i" is used. The parameter "n" is the number of wheels in an aircraft. The drag calculation for the strut of landing gear is presented in the next Section. Some aircraft are equipped with skid, especially when they have tail gear configuration. Skid is not a lifting surface, but for the purpose of zero-lift drag calculation, it may be treated as a small wing.

3.4.5. Strut

In this section, we deal with two types of strut: 1. Landing gear strut, and 2. wing strut. Landing gear is often attached to the aircraft structure via strut. In some GA/homebuilt aircraft, wings are attached through a few struts to support wing structure; i.e., strut-braced (see figure 3.14). Modern aircraft use advanced material for structure that are stronger and there are no need for any strut to support their wings; i.e. cantilever. In some aircraft (such as hang gliders), the cross section of the wing strut is a symmetrical airfoil in order to reduce the strut drag. In both cases, the strut is producing an extra drag for aircraft.

The increase in C_{Do} due to application of strut is given by the following empirical equation:

$$C_{D_{o_s}} = \sum_{i=1}^{n} C_{D_{o_{s_i}}} \left(\frac{S_s}{S} \right)$$

<div align="right">(3.31)</div>

where S_s is the frontal area of each strut (its diameter times its length), and S is the wing reference area. The parameter C_{Dos} is the drag coefficient of each strut; that is 0.1, when it is faired (i.e., has an airfoil section). When strut does not have an airfoil section, its drag coefficient is obtained from Table 3.1. The parameter "n" is the number of struts in an aircraft. It is observed that using an airfoil section for a strut decreases its drag by an order of 10. However, its manufacturing cost is increased too.

Figure 3.14. *Wing strut and landing gear strut in a Cessna 172*

3.4.6. Nacelle

If the engine is not buried inside fuselage, it must be in a direct contact with air flow. In order to reduce the engine drag, engine is often located inside an aerodynamic cover called nacelle. For the purpose of drag calculation, it can be considered that the nacelle is similar to the fuselage, except its length-to-diameter ratio is lower. Thus, the nacelle zero-lift drag coefficient (C_{Don}) will be determined in the same way as in a fuselage. In the case where the nacelle length-to-diameter ratio is below 2, assume 2. This parameter is used in the equation 3.17. Some aero-engine manufacturers publish the engine nacelle drag in the engine catalog, when the installed drag is demonstrated. In such case, use that manufacturer data. Determine nacelle drag, only when the engine uninstall thrust is available.

3.4.7. External Fuel Tank

An external fuel tank (such as a wingtip tank) is in a direct contact with air flow and is generating drag. An external fuel tank may be modeled as a small fuselage. In the case where the fuel tank length-to-diameter ratio is below 2, assume 2.

3.4.8. Cooling Drag

An aeroengine is a source of heat where it is generated when fuel is burned in the combustion chamber. This heat is initially conducted to the engine external surface such including cylinder heads via oil/water. In order to keep the engine efficient and maintain its performance, the heat should be transferred to outside airflow through a convenient technique; usually conduction. Various types of heat exchangers are arranged in an aeroengine which require a flow of air through them for the purposes of cooling. The source of this cooling air is usually the free air stream possibly augmented to some extent by a propeller slipstream (in a prop-driven engine) or bleed from the compressor section (in a turbine engine).

As the air flows through, to extract heat energy from the body, it experiences a loss in the total pressure and momentum. This loss during heat transfer process may be interpreted as a drag force referred to as the cooling drag.

Turbine engine manufacturers calculate the net power/thrust lost in the flow and subtract this from the engine uninstalled power/thrust. In such case, no cooling drag increment is added to the aircraft. Piston engine manufacturer often does not provide installed power, so the cooling drag needs to be determined in order to calculate the installed power. For a piston engine, the engine power is typically reduced by as much as approximately 5% to account for the cooling losses.
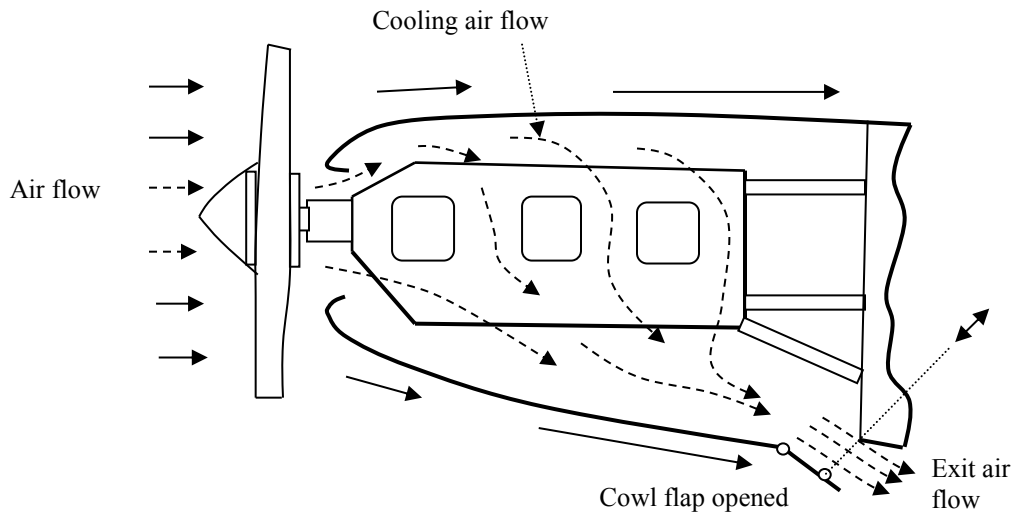
Figure 3.15. The use of cowl flaps to control engine cooling air

An engine needs to be installed to the aircraft structure (e.g., fuselage and wing) through a special mounting/pylon. An air cooled engine has a special mounting (See figure 3.15) to provide the airflow around the engine. The calculation of the cooling drag is highly installation-dependent. It is unfeasible to present a general technique which can be applied to every engine installation. Turbine/Piston engines manufacturers use

computer software packages for the calculation of installation losses for their engines. Because of the complexity of the engine configuration and the internal flow through a typical engine installation, current methods for estimating cooling losses are empirical in nature.

For an oil-cooled turbine engine, it is sufficient to consider cooling drag by consulting with the engine manufacturer catalog and using installed power/thrust. For an air-cooled engine, engine cooling drag coefficient (C_{Doen}) is given [14] by the following empirical relationship:

$$C_{D_{o_{en}}} = 4.51 \times 10^{-8} \frac{K_e P T^2}{\sigma V S} \tag{3.32}$$

where P is the engine power (in hp), T is the hot air temperature (in K) at exit, σ is the relative density of the air, V is the aircraft airspeed (in m/sec), and S is the wing reference area (in m^2). The parameter K_e is a coefficient that depends on the type of engine and its installation. It varies between 1 and 3.

3.4.9. Trim Drag

Basically, trim drag is not basically different from the types of drag already discussed. It arises mainly as the result of having to produce a horizontal tail load in order to balance the airplane around its center of gravity. Any drag increment that can be attributed to a finite lift on the horizontal tail contributes to the trim drag. Such increments mainly represent changes in the induced drag of the tail.

To examine this further, we begin with the sum of the lifts developed by the wing and tail that must be equal with the aircraft weight in a trimmed cruising flight.

$$L_t + L_w = L = W \tag{3.33}$$

where

$$L_w = \frac{1}{2} \rho V^2 S_w C_{L_w} \tag{3.34}$$

$$L_t = \frac{1}{2} \rho V^2 S_t C_{L_t} \tag{3.35}$$

Equation 3.33 is one of the requirements of the aircraft longitudinal trim requirements in cruising flight. Substituting tail and wing lift into equation 3.33, one can derive the horizontal tail lift coefficient (C_{Lt}) as:

$$C_{L_t} = \left(C_L - C_{L_w} \right) \frac{S}{S_t} \tag{3.36}$$

where C_L is aircraft lift coefficient, C_{Lw} is wing lift coefficient, and S_t is horizontal tail area. Then, the trim drag will be:

$$C_{D_{o_{trim}}} = C_{D_{i_t}} = K_t C_{L_t}^2 \frac{S_t}{S} = \frac{1}{\pi \cdot e_t \cdot AR_t} \frac{S_t}{S} \left[\left(C_L - C_{L_w} \right) \frac{S}{S_t} \right]^2 \tag{3.37}$$

where e_t is horizontal tail span Oswald efficiency factor, and AR_t is the horizontal tail aspect ratio. The trim drag is usually small, amounting to only 1% or 2% of the total drag of an airplane for the cruise condition. Reference 5, for example, lists the trim drag for the Learjet Model 25 as being only 1.5% of the total drag for the cruise condition.

3.4.10. C_{D_0} of Other Parts and Components

So far, we introduced techniques to calculate C_{D_0} of aircraft major components. There are other components, parts, factors, and items that are producing drag and contribute to total the C_{D_0} of an aircraft. These items are introduced in this subsection.

1. Interference

When two bodies intersect or are placed in proximity, their pressure distributions and boundary layers can interact with each other, resulting in a net drag of the combination that is often higher than the sum of the separate drags. This increment in the drag is known as interference drag. Except for specific cases where data are available, interference drag is difficult to calculate accurately. Four examples are: 1. placing an engine nacelle in proximity to a rear pylon (e.g., Gulfstream V), and 2. the interference drag between the wing and fuselage in a mid-wing configuration. 3. horizontal tail aft of jet engine exhaust nozzle, and 4. wing leading edge aft of a propeller wake.

a. High wing   Interference   *b. Mid wing*

c. Low wing   *d. Parasol wing*
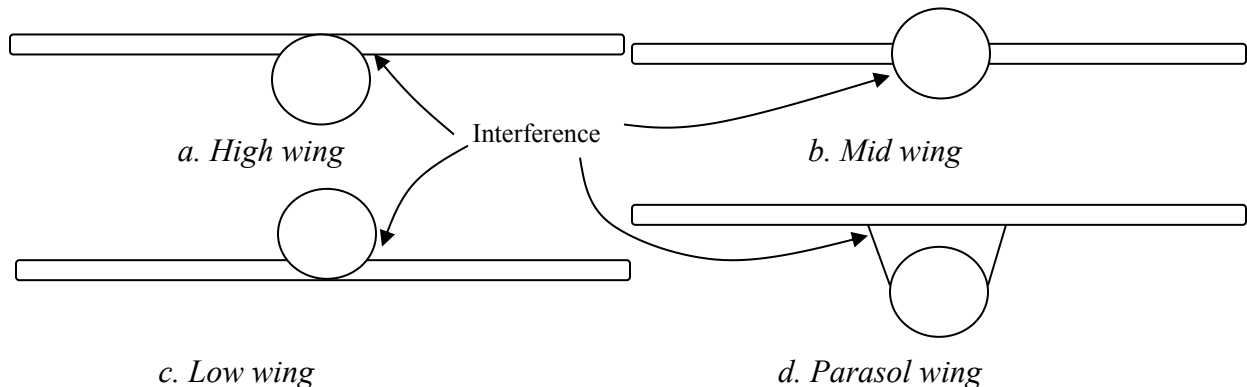
Figure 3.16. *Wing-fuselage interference drag*

Figure 3.16 shows a wing attached to the side of a fuselage. At the fuselage-wing juncture a drag increment results as the boundary layers from the two components interact and thicken locally at the junction. This type of drag penalty will become more severe if surfaces meet at an angle other than 90°. Reference [4] shows that the interference drag of a strut attached to a body doubles as the angle decreases from 90° to approximately 60°. Avoid acute angles, if not, filleting should be applied at the juncture to reduce interference drag.

In the case of a high-wing configuration, interference drag results principally from the interaction of the fuselage boundary layer with that from the wing's lower surface. This latter layer is relatively thin at positive angles of attack. In addition, it is the boundary layer on the upper surface of a low wing that interferes with the fuselage boundary layer. The upper surface boundary layer is relatively thicker than the lower

surface boundary layer. Thus, the wing-fuselage interference drag for a low-wing aircraft is usually greater than for a high-wing aircraft.

The available data on interference drag are limited; References [2] and [4] presents a limited amount. Based on this reference, an approximate drag increment caused by wing-fuselage interference is estimated to equal 4% of the wing's zero-lift drag for a typical aspect ratio and wing thickness.

Theoretical accurate calculation of interference drag is impossible, unless you utilize a high fidelity computational fluid dynamics (CFD) software package. For example, a wing protruding from a fuselage just forward of the station where the fuselage begins to taper may trigger a flow separation over the rear portion of the fuselage. Sometimes interference drag can be favorable as, for example, when one body operates in the wake of another. The most accurate technique to determine interference drag is to employ wind tunnel or flight test.

2. Antenna
The communication antennas of many aircraft are located outside of the aircraft. They are in direct contact with the air, hence they produce drag. There are mainly two types of antennas: a. rod or wire, and b. blade or plate. Both type of antennas should be in an open space (below on above the fuselage) for a better communication. During a flight, airstream flows around an antenna, so it will generate drag.

Figure 3.17. *The UHF radio antenna of a reconnaissance aircraft U-2S Dragon Lady*

Figure 3.18. Antenna of Boeing Vertol CH-113 Labrador

Figure 3.17 shows a rod antenna of reconnaissance aircraft U-2S Dragon Lady. The large plate antenna of a reconnaissance aircraft U-2S is the UHF radio antenna. The thin whip acts as an ADF antenna. The whip was originally straight. The bend in the upper portion of the whip antenna was introduced to provide clearance for the senior span/spur dorsal pod. Most reconnaissance aircraft U-2 seem to now use the bent whip, even if they are not capable of carrying the senior span/spur dorsal pod.

Figure 3.18 illustrates lower fuselage section of a Boeing Vertol CH-113 Labrador with various antennas and plates. Note the two blade antennas, and two whip antennas. Also seen, is the towel-rack 'loran' antenna. The item hanging down, in the distance, is the sectioned flat plate that covers the ramp hinge, when the ramp is closed.

a.   pitot tube mounted under the wing of a Cessna 172

b.   Boeing 767 fuselage nose with three pitot tubes [16]
Figure 3.19. pitot tube

To calculate C_{D_o} of antenna, rod antenna is treated as a strut, and blade antenna is considered as a small wing. The very equations that are introduced for strut (Section 3.4.5) and wing (Section 3.4.2) may be employed to determine the C_{D_o} of an antenna.

3. Pitot Tube

A pitot tube (combined with a static port) is a pressure measurement instrument used to measure airspeed and sometimes altitude of an aircraft (see figure 3.19). The basic pitot tube simply consists of a tube pointing directly into the air flow. As this tube contains air, a pressure can be measured as the moving air is brought to rest. This pressure is stagnation pressure of the air, also known as the total pressure, or sometimes the pitot pressure.

Since the pitot tube is in direct contact with the outside air, it has a contribution to aircraft drag (i.e., C_{D_o}). If the aircraft is in subsonic regime, the horizontal part of the pitot tube may be assumed as a little fuselage and its vertical part as a strut. In a supersonic flight, shock wave is formed around a pitot tube, and creates additional wave drag. For supersonic flow, section 3.5 introduces a technique to account for pitot tube zero-lift drag coefficient (C_{D_o}).

4. Surface Roughness

The outer surface of an aircraft structure (skin) has a considerable role in aircraft drag. For this reason, the aircraft skin is often finished and painted. The paint not only protects the skin from atmospheric hazards (e.g., rusting), but also reduces its drag. As the surface of the skin is more polished, the aircraft drag (surface friction) will be reduced. The interested reader is referred to specific aerodynamic references and published journal papers to obtain more information about the effect of surface roughness on the aircraft drag.

5. Leakage

There are usually gaps between control surfaces (such as elevator, aileron and rudder), flaps, and spoilers and the lifting surfaces (such as wing and tails). The air is flowing through these tiny gaps and thus producing extra drag. This is called leakage drag. Leakage drag is usually contributing about 1% - 2% to total drag. The reader is referred to specific aerodynamic references and published journal papers to gain more information about the influence of these gaps on the aircraft drag.

6. Rivet and Screw

The outside of the aircraft structure (fuselage and wing) is covered with a skin. The skin; if it is from metallic materials; is attached to the primary components of an aircraft structure (such as spar and frame) via parts such as rivets or screws. The Composite structures have the advantage that they do not require any rivet or screw, and are often attached together through techniques such as bonding.

In the case of the screw, the top part of the screw could be often hidden inside skin. But the heads of most types of rivets are out of skin, therefore they produce extra drag. Figure 3.19a illustrates both rivet and screw on wing of Cessna-172. Rivets and

---

screws are usually contributing about 2% -3% to total drag. The author did not find any reference which demonstrates the calculation of rivet contribution to aircraft drag. you may use flight test to measure this type of drag.

7. Pylon

A podded turbine engine (e.g., turbofan engine) is usually mounted to the airplane wing or fuselage with a pylon. Pylon is mainly a structural component, but may be designed such that it contributes to aircraft lift. Although pylon is not fundamentally a lifting surface, but for the purpose of zero-lift drag calculation, it may be treated as a small wing.

8. Compressibility

Compressibility effects on aircraft drag have been important since the advent of high-speed aircraft in the 1940s. Compressibility is a property of the fluid, when a fluid is compressed, its density will be increased. Liquids have very low values of compressibility whereas gases have high compressibility. In real life, every flow of every fluid is compressible to some greater or lesser extent. A truly constant density (incompressible) fluid is a myth. However, for almost all liquids (e.g., water), the density changes are so small that the assumption of constant density can be made with reasonable accuracy.
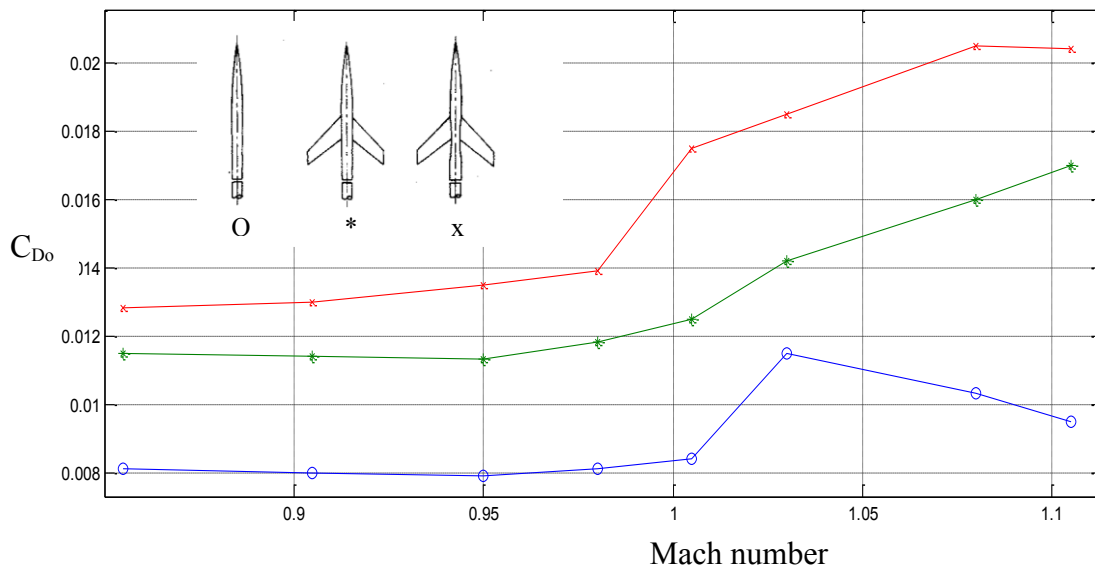
Figure 3.20. *Drag rise due to compressibility for swept wing-body combinations (Ref. 1)*

As a fluid is compressible, a flow of fluid may be compressible too. Incompressible flow is a flow where the density is assumed to be constant throughout. Compressible flow is a flow in which the density is varying. A few important examples are the internal flows through rocket and gas turbine engines, high-speed subsonic, transonic, supersonic, and hypersonic wind tunnels, the external flow over modern airplanes designed to cruise faster than Mach 0.3, and the flow inside the common

internal combustion reciprocating engine. For most practical problems, if the density changes by more than 5 percent, the flow is considered to be compressible. Figure 3.20 shows the effect of compressibility on drag for three configurations.

Flow velocities higher than Mach 0.3 are associated with a considerable pressure changes, accompanied by correspondingly noticeable changes in density. The aircraft drag at high subsonic speed (e.g., M = 0.9) is about twice as of that at low subsonic speed (e.g., Mach 0.2). Consider a wing with a free stream. The lift is created by the occurrence of pressure higher than free stream on the lower surface of the wing and lower than free stream on the upper surface. The is usually coincides by the occurrence of velocities higher than free stream on the upper surface of the wing and lower than free stream on much of the lower surface.

As the airspeed approaches the speed of sound (i.e., M > 0.85), due to a positive camber, the higher local velocities on the upper surface of the wing may reach and even substantially exceed local sonic speed, M = 1 (See Figure 3.21). The free stream Mach number at which the maximum local Mach number reaches 1 is referred to as the critical Mach number.
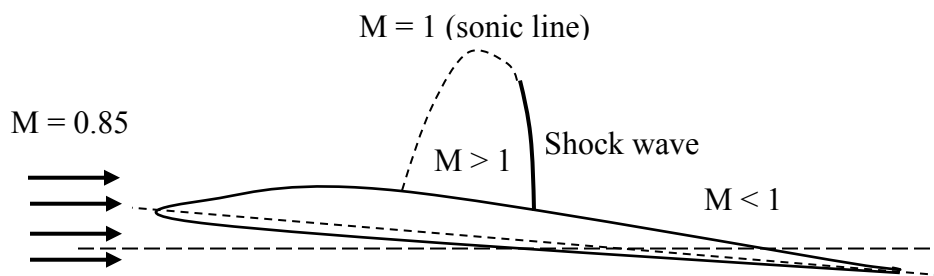

Figure 3.21. Local supersonic speed with a high subsonic flow

The existence of sonic and supersonic local velocities on a wing is associated with an increase in drag. The extra drag is due to a reduction in total pressure through oblique shock wave which causes local adverse pressure gradients. In addition, when an oblique shock interacts with boundary layer, the boundary layer gets thicker and may even separates. This is referred to as compressibility drag.

A cambered airfoil has typically a crest and a lifting surface with such airfoil has a crestline. The *crest* is the point on the airfoil upper surface to which the free stream is tangent. The crestline is the locus of airfoil crests along the wing span. The drag increase due to compressibility is generally not large, until the local speed of sound occurs at or behind the crest of the airfoil. Empirically, it is found for all airfoils except the supercritical airfoil, that at 2% to 4% higher Mach number than that at which M = 1 at the crest the drag rises abruptly. The Mach number at which this abrupt drag rise begins is called the *Drag Divergence Mach number*.
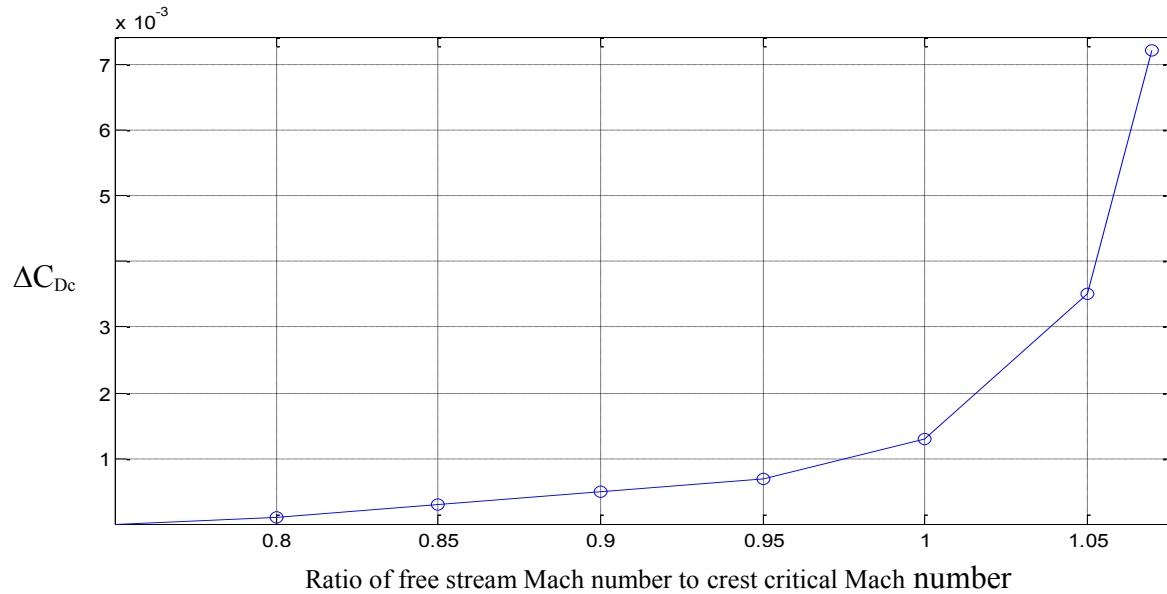
Figure 3.22. *Incremental drag coefficient due to compressibility (Ref. 1)*

However, the occurrence of substantial supersonic local velocities well ahead of the crest does not lead to a significant drag increase provided that the velocities decrease again below sonic speed forward of the crest. The incremental drag coefficient due to compressibility is designated ΔC_{Dc}. Figure 3.22 is an empirical average of existing transport aircraft data. Table 3.4 demonstrates the incremental drag coefficient due to compressibility for several aircraft.

No	Aircraft	C_{Do} at low subsonic speed	C_{Do} at high subsonic speed	Incremental drag coefficient due to compressibility (ΔC_{Dc})
1	Boeing 727	0.017	0.03	76.5%
2	North American F-86 Sabre	0.014	0.04	207.7%
3	Grumman F-14 Tomcat	0.021	0.029	38.1%
4	McDonnell Douglas F-4 Phantom	0.022	0.031	40.9%
5	Convair F-106 Delta Dart	0.013	0.02	54%

Table 3.4. Drag increase due to compressibility effects for several aircraft

A complete set of drag curves for a typical large transport jet is given in Figure 3.23.

9. Miscellaneous items

There are other items which produce drag, but due to their variations, were not listed in this section. These include such items as 1. footstep in small GA aircraft which allow the pilot or technician to climb up; 2. small plate on tails to balance the manufacturing unbalances, 3. catapult hook, 4. pipe and funnel for aerial fuel refueling, 5. wiper blades, 6. angle of attack meter vane, 7. non-streamlined fuselage, 8. deflector cable, 9. chemical

sprayer in agricultural aircraft, 10. vortex generator, 11. navigation lights, and 12. fitting. The calculation of drag of such minor items is out of scope of this text.
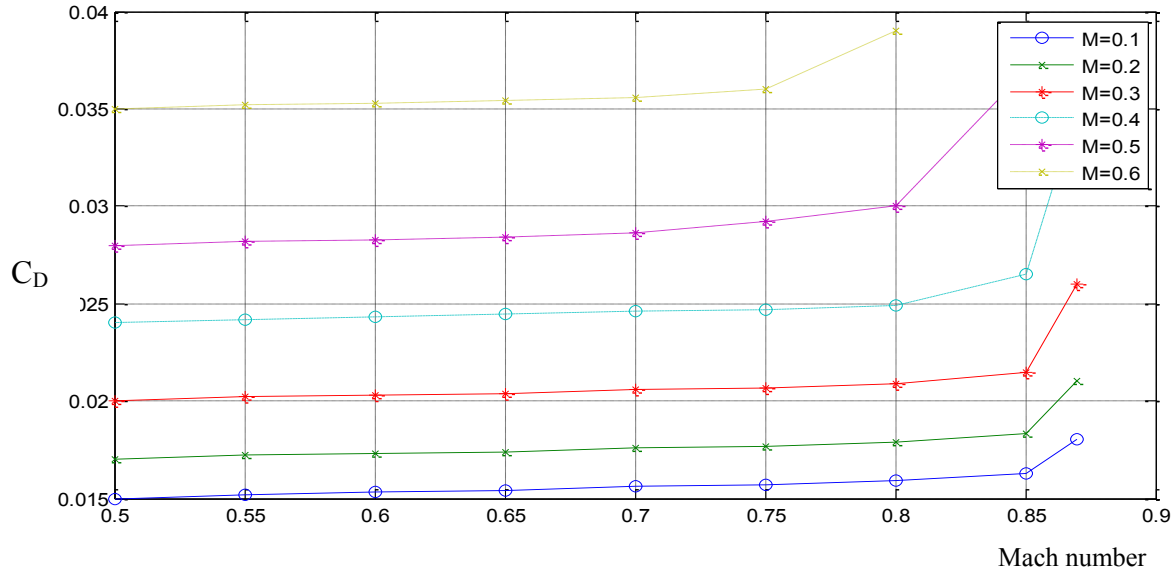

Figure 3.23. *Drag coefficient versus Mach number*

3.4.10. Overall C_{Do}

Based on the build-up technique, the overall C_{Do} is determined readily as the sum of C_{Do} of all aircraft components and factors. The calculation of C_{Do} contribution due to factors as introduced in section 3.4.9 is complicated. These factors sometimes are responsible for an increase in C_{Do} up to about 50%. Thus we will resort to a correction factor in our calculation technique. Then, the overall C_{Do} of an aircraft is given by:

$$C_{D_o} = K_c \left[C_{D_{o_w}} + C_{D_{o_f}} + C_{D_{o_{ht}}} + C_{D_{o_{vt}}} + C_{D_{o_s}} + C_{D_{o_{lg}}} + C_{D_{o_n}} + C_{D_{o_{fi}}} + ... \right] \qquad (3.38)$$

No	Aircraft type	K_c
1	Jet transport	1.1
2	Agriculture	1.5
3	Prop Driven Cargo	1.2
4	Single engine piston	1.3
5	General Aviation	1.2
6	Fighter	1.1
7	Glider	1.05
8	Remote Controlled	1.2

Table 3.5. *Correction factor (K_c) for equation 3.38*

where K_c is a correction factor and depends on several factors such as the type, year of fabrication, degree of streamline-ness of fuselage, configuration of the aircraft, and number of miscellaneous items. Table 3.5 yields the K_c for several types of aircraft.

Each component has a contribution to overall C_{Do} of an aircraft. Their contributions vary from aircraft to aircraft and from configuration to configuration (e.g., cruise to take-off). Table 3.6 illustrates [2] contributions of all major components of Gates Learjet 25 to aircraft C_{Do}. Note that the row 8 of this table shows the contributions of other components as high as 20%.

No	Component	C_{Do} of component	Percent from total C_{Do} (%)
1	Wing	0.0053	23.4
2	Fuselage	0.0063	27.8
3	Wing tip tank	0.0021	9.3
4	Nacelle	0.0012	5.3
5	Engine strut	0.0003	1.3
6	Horizontal tail	0.0016	7.1
7	Vertical tail	0.0011	4.8
8	Other components	0.0046	20.4
9	Total C_{Do}	**0.0226**	100

Table 3.6. *C_{Do} of major components of Gates Learjet 25*

No	Aircraft	Type	Landing gear	m_{TO} (kg)	S (m^2)	Engine	C_{Do}
1	Cessna 172	Single engine GA	Fixed	1,111	16.2	Piston	0.028
2	Cessna 182	Single engine GA	Fixed	1,406	16.2	Piston	0.029
3	Cessna 185	Single engine GA	Fixed	1,520	16.2	Piston	0.021
4	Cessna 310	Twin engine GA	Retractable	2,087		Piston	0.026
5	Learjet 25	Business jet	Retractable	6,804	21.53	2 Turbojet	0.0226
6	Gulfstream II	Business jet	Retractable	29,711	75.21	2 Turbofan	0.023
7	Saab 340	Transport	Retractable	29,000	41.81	2 Turboprop	0.028
8	McDonnell Douglas D-C-9-30	Airliner	Retractable	49,090	92.97	2 Turbofan	0.021
9	Boeing 707-320	Airliner	Retractable	151,320		4 Turbofan	0.013
10	Boeing 767-200	Airliner	Retractable	142,880	283.3	2 Turbofan	0.0135
11	Airbus 340-200	Airliner	Retractable	275,000	361.6	4 Turbofan	0.0165
12	Boeing C-17 Globemaster III	Transport	Retractable	265,350	353	4 Turbofan	0.0175

Table 3.7. C_{Do} of several aircraft at low speed

Table 3.7 illustrates C_{Do} of several aircraft at low speeds [15]. The retired airliner Boeing 707 was a very aerodynamic aircraft with a C_{Do} of 0.013. You may have noticed that Cessna 185 has a lower C_{Do} compared with Cessna 172 and Cessna 182. The reason is

that Cessna 172 and Cessna 182 are equipped with fixed tricycle landing gear while Cessna 185 has a fixed tail dragger.

3.5. Wave Drag

In supersonic airspeeds, a new type of drag is produced and it is referred to as "shock wave drag" or simply "wave drag". When a supersonic flow experiences an obstacle (e.g., wing leading edge or fuselage nose); it is turned into itself and a shock wave is formed. A shock wave is a thin sheet of air across which abrupt changes occur in flow parameters such as pressure, temperature, density, speed, and Mach number. In general, air flowing through a shock wave experiences a jump toward higher density, higher pressure, higher temperature, and lower Mach number. The effective Mach number approaching the shock wave is the Mach number of the component of velocity normal to the shock wave. This component Mach number must be greater than 1.0 for a shock to exist. The wave drag; the new source of drag; is inherently related to the loss of the stagnation pressure and increase of entropy across the oblique and normal shock waves.

In general, a shock wave is always required to bring supersonic flow back to subsonic regime. In a subsonic free stream, whenever the local Mach number becomes greater than 1 over the surface of a wing or body, the flow must be decelerated to a subsonic speed before reaching the trailing edge. If the surface could be shaped such that the surface Mach number is reduced to 1 and then decelerated subsonically to reach the trailing edge at the surrounding free stream pressure, there would be no shock wave and no shock drag. A major goal of transonic airfoil design is to reduce the local supersonic Mach number to as close to 1 as possible before the shock wave. One of the main functions of sweep angle in a swept wing is to reduce wave drag at transonic and supersonic airspeeds.

In supersonic airspeeds, three main types of waves are created: 1. oblique shock wave, 2. normal shock wave, and 3. Expansion waves. In general, an oblique shock wave brings a supersonic flow to another supersonic flow with a lower Mach number. A normal shock wave brings a supersonic flow to a subsonic flow (i.e., Mach number less than 1). However, an expansion wave brings a supersonic flow to another supersonic flow with a higher Mach number. In supersonic airspeeds, a shock wave may happen at any place in the aircraft, including wing leading edge, horizontal tail leading edge, vertical tail leading edge, and engine inlet. All these aircraft components locations will create an extra drag when a shock wave is formed. Thus, in supersonic speed, the drag coefficient is expressed by:

$$C_D = C_{D_o} + C_{D_i} + C_{D_w} \tag{3.39}$$

where C_{Dw} is referred to as "wave drag coefficient". The precise calculation of C_{Dw} is time consuming, but to give the reader the guidance, we present two techniques, one for a lifting surface leading edge; and one for the whole aircraft. For a complicated geometry aircraft configuration, the drag may be computed with aerodynamics techniques such as vortex panel method and *Computational Fluid Dynamics*" techniques. Figure 3.24 illustrates Lockheed Martin F-35 Lightning Joint Strike Fighter, a new generation of

fighters. It is claimed that F-35 will be the last manned fighters, and in the near future, the fighters will be unmanned.

Figure 3.24. Lockheed Martin F-35 Lightning Joint Strike Fighter, a new generation of fighters

3.5.1. Wave Drag for Wing and Tail

In this section, the wave drag of a wing is presented. In an aircraft with a supersonic maximum speed, the locations where have the first impact with airflow (such as wing leading edge, horizontal tail leading edge, vertical tail leading edge, fuselage nose, and engine inlet edge) are usually made sharp. One main reason for this initiative is to reduce the number of shack waves created over the aircraft components during a supersonic flight. Two airfoil cross sections which are frequently employed for wing, horizontal tail, and vertical tail are double wedge and biconvex (See figure 3.25).
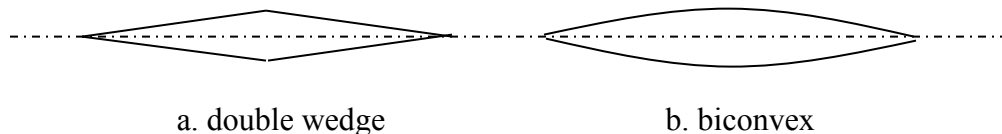
a. double wedge   b. biconvex
Figure 3.25. Supersonic airfoil sections

In this section, a wave drag calculation technique is introduced which is applicable to any component where has a corner angle (e.g., double wedge and biconvex) and experiences a shock wave. Then wave drag coefficient (C_{Dw}) for such component is calculated separately and then all C_{Dw} are summed together.

Consider a the front top half of a wedge with a sharp corner that experiences an oblique shock in a supersonic flow (as illustrated in Figure 3.26). The wedge has a wedge angle of θ, and the free stream pressure, and Mach number are P_1 and M_1 respectively. When

the supersonic flow hits the corner, an oblique shock with angle of β to the free stream is generated.

For each component with such configuration, the wave drag coefficient is given by:

$$C_{D_w} = \frac{D_w}{\frac{1}{2}\rho V_\infty^2 S} = \frac{D_w}{\frac{1}{2}\gamma \cdot M^2 PS}$$ (3.40)

where subscript infinity (∞) means that the parameter are considered in the infinity distance from the surface. Please note that, this does not really mean infinity, but it simply means at a distance out of the effect of shock and the surface (i.e., free stream). The parameter S is the surface of a body at which the pressure is acting (i.e., planform area).

D_w is the wave drag and is equal to the axial component of the pressure force. In supersonic speeds, the induced drag may be ignored, since it has negligible contribution, compared to the wave drag. In supersonic speeds, the lift coefficient has a very low value. Since, the wedge has an angle, θ; the drag force due to flow pressure actin on a wedge surface with an area of "A" is given by:

$$D_w = P_2 A(\sin\theta)$$ (3.41)

where P_2 represents the pressure behind an oblique shock wave, and θ is the corner angle (see figure 3.26). Please note that; in this particular case, the pressure at the lower surface is not changed. The relationship between upstream and downstream flow parameters may be derived using energy law, mass conservation law, and momentum equation. The relationship between upstream pressure (P_1) and downstream pressure (P_2) is given [7] by:

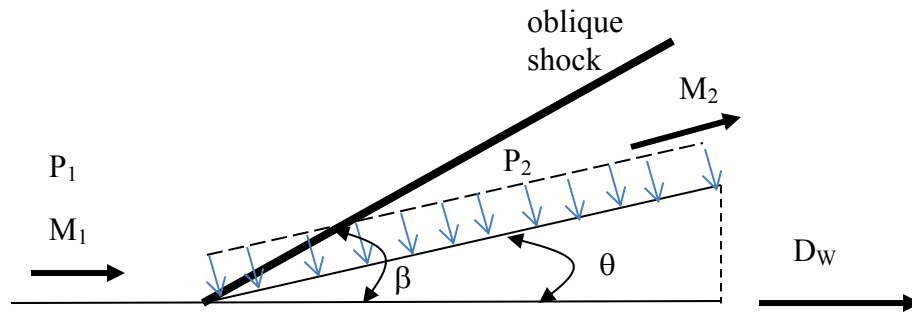Figure 3.26. *Geometry for drag wave over a wedge*

$$P_2 = P_1\left[1 + \frac{2\gamma}{\gamma+1}\left(M_{n1}^2 - 1\right)\right]$$ (3.42)

where γ is the is the ratio of specific heats at constant pressure and constant volume (γ = c_p/c_v). For air at standard condition, γ is 1.4. The variable M_{n1} is the normal component of the upstream Mach number, and is given by:

$$M_{n1} = M_1 \sin \beta \tag{3.43}$$

The parameter β (oblique shock angle) is a nonlinear function of upstream Mach number and wedge corner angle (θ):

$$\tan \theta = 2 \cot \beta \left[\frac{M_1^2 \sin^2 \beta - 1}{M_1^2 (\gamma + \cos 2\beta) + 2} \right] \tag{3.44}$$

Equation 3.44 is called θ–β-M relation. For any given θ, there are two values of β predicted for any given Mach number. Take the lower value which is the representation of the weal shock wave which is favored by the nature.

The pressure may also be non-dimensionalized as follows:

$$P_2 - P_\infty = \frac{1}{2} \rho_\infty V_\infty^2 C_p = \frac{1}{2} \gamma \cdot M_\infty^2 P_\infty C_p \tag{3.45}$$

where C_p is the pressure coefficient.

Now, consider another more general case, where a supersonic airfoil has an angle of attack, or when the second half of a wedge is considered. In such a case, where a supersonic flow is turned away from itself, an expansion wave is formed (See figure 3.27). Expansion waves are the antithesis of shock waves. In an expansion corner, the flow Mach number is increased, but the static pressure, air density, and temperature decrease through an expansion wave. The expansion wave is also referred to as the Prandtl-Meyer expansion wave.
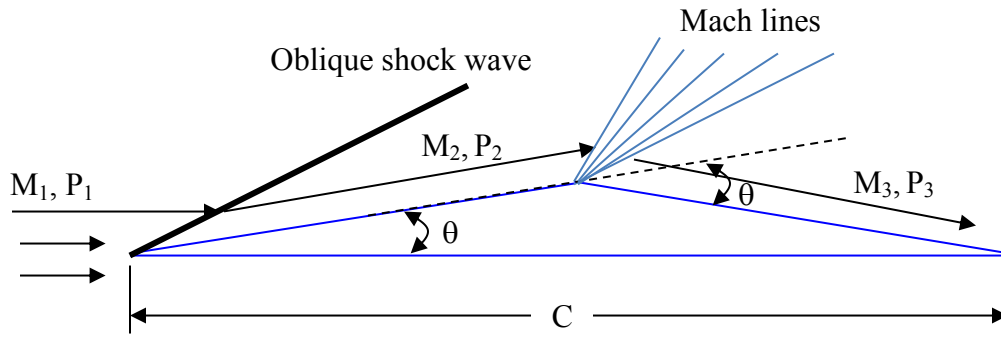
Figure 3.27. Oblique shock and Prandtl-Meyer expansion waves

For a wing with a wedge airfoil section shown in figure 3.27, the drag force is the horizontal components of the pressure force, so:

$$D = P_2 A \sin \theta - P_3 A \sin \theta \tag{3.46}$$

where A is the surface area, and is equal to:

$$A = b \frac{C/2}{\cos \theta} \tag{3.47}$$

where b is the wing span (not shown in the figure). Plugging the equation 3.46 into equation 3.47, the following result is obtained:

$$D = (P_2 - P_3)b \frac{C/2}{\cos \theta} \sin \theta = \frac{1}{2}(P_2 - P_3)bC \tan \theta \tag{3.48}$$

If the wing has a different geometry, use this basic technique to determine the wing wave drag. The pressure behind the expansion wave is given [7] by the following equation:

$$P_3 = P_2 \left[\frac{1 + \frac{\gamma - 1}{2} M_2^2}{1 + \frac{\gamma - 1}{2} M_3^2} \right]^{\frac{\gamma}{\gamma - 1}} \tag{3.49}$$

where the flow Mach number behind expansion wave (M_3) and the flow Mach number behind expansion wave (M_2) are related through the turn angle, θ :

$$\theta = v(M_3) - v(M_2) \tag{3.50}$$

The $v(M)$ is referred to as the Prandtl-Meyer function and is given by:

$$v(M) = \sqrt{\frac{\gamma + 1}{\gamma - 1}} \tan^{-1} \left[\sqrt{\frac{\gamma - 1}{\gamma + 1}(M^2 - 1)} \right] - \tan^{-1} \left[\sqrt{(M^2 - 1)} \right] \tag{3.51}$$

The equation 3.51 should be employed twice in the calculation; once to calculate M_2, and once to determine M_3. Example 3.3 indicates the application of the technique.
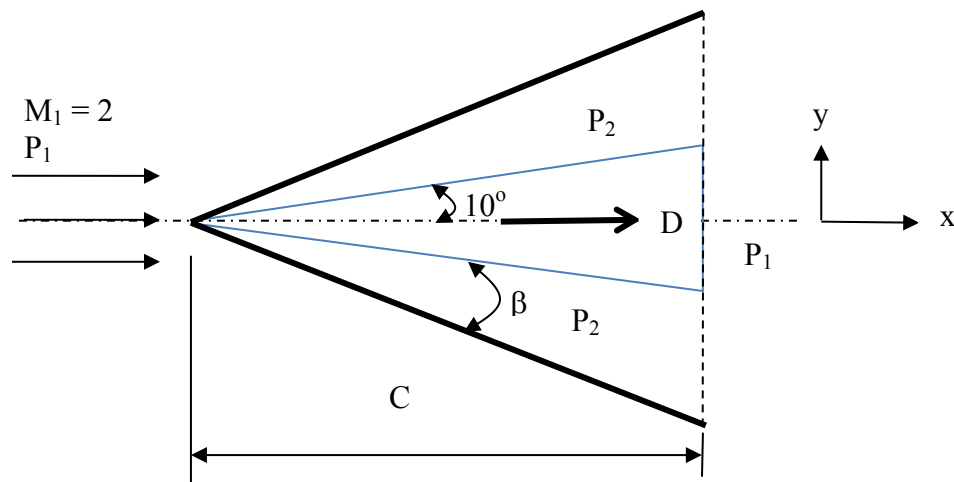

Example 3.2:

Figure 3.28. Geometry for Example 3.2 (side-view)

Consider a rectangular wing with a span; b (not shown in the figure) of 5 m and a chord; C of 2 m in a Mach 2 air flow (the side-view is sketched in figure 3.28). The airfoil

section is a 10° half-angle wedge at zero angle of attack. Calculate the wave drag coefficient. Assume that the expansion over the corners of the base is such that, the base pressure is equal to the free-stream pressure. The experiment is performed at sea level ISA condition.

Solution:
At sea level ISA condition, the free-stream pressure is 1 atm (i.e., 101,325 Pa), and air density is 1.225 kg/m^3. The ratio of specific heats at constant pressure and constant volume for air, γ is 1.4. Since the supersonic flow turns to itself, an oblique shock wave is produced both at top and bottom surfaces. Pressure is increased behind the shock wave (P_2). In order to determine the pressure P_2, we need to first calculate the shock wave angle (β):

$$\tan\theta = 2\cot\beta\left[\frac{M_1^2\sin^2\beta - 1}{M_1^2(\gamma + \cos 2\beta) + 2}\right] \Rightarrow \tan(10) = 2\cot\beta\left[\frac{2^2\sin^2\beta - 1}{2^2(1.4 + \cos 2\beta) + 2}\right] \quad (3.44)$$

The solution of this nonlinear equation yields an angle of 39.3 degrees (β = 39.3 deg). The normal component to the shock M_{n1} is:
$$M_{n1} = M_1\sin\beta = 2\sin(39.3) = 1.27 \quad (3.43)$$
The static pressure behind the shock wave is:

$$P_2 = P_1\left[1 + \frac{2\gamma}{\gamma + 1}(M_{n1}^2 - 1)\right] = 101,325\left[1 + \frac{2(1.4)}{1.4 + 1}(1.27^2 - 1)\right] \quad (3.42)$$

$$\Rightarrow P_2 = 172,364 \quad Pa$$

The wave drag is the net force in the x direction; P_2 is exerted perpendicular to the top and bottom surfaces. The force due to P_1 exerted over the base is in the direction opposite to the x axis. S is the planform area (the projected area seen by viewing the wedge from the top, thus S = c × b. The drag, D_w, is the summation of two top and bottom pressure force (see Figure 3.29) components in x direction, minus the force from base pressure:
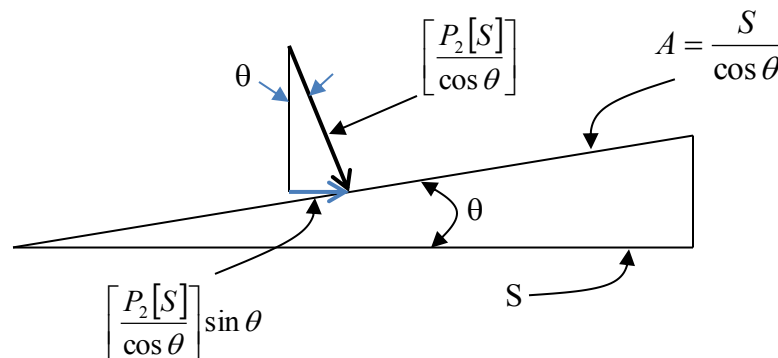
Figure 3.29. Wave drag, the component of pressure force in x direction

$$D_w = 2P_2A_2(\sin\theta) - P_1A_1 \quad (3.41)$$

where A_2 is the base area, and A_1 is the top and bottom surfaces:

$$A_1 = 2bC\tan(10)$$

$$A_2 = b\frac{C}{\cos(10)}$$

Thus:

$$D_w = 2P_2\left[b\frac{C}{\cos 10}\right]\sin(10) - P_1b[2C\tan(10)]$$

$$D_w == 2\times 172{,}364\times 5\times 2\times\tan(10) - 2\times 110{,}325\times 5\times 2\times\tan(10) = 251{,}670 \quad N$$

By definition, the wave drag coefficient is:

$$C_{D_w} = \frac{D_w}{\frac{1}{2}\gamma\cdot M_\infty^2 P_\infty S} = \frac{251{,}670}{0.5\times 1.4\times 101{,}325\times 2^2\times 5\times 2} \tag{3.40}$$

$$\Rightarrow C_{D_w} = 0.089$$

Note that this drag coefficient is based on the shock wave, and it includes the contribution of the base.

Example 3.3:

Consider a very thin flat plate wing with a chord of 2 m and a span of 5 m. The wing is placed at a 5° angle of attack in a Mach 2.5 air flow (Figure 3.30). Determine the wave drag coefficient. Assume sea level ISA condition.
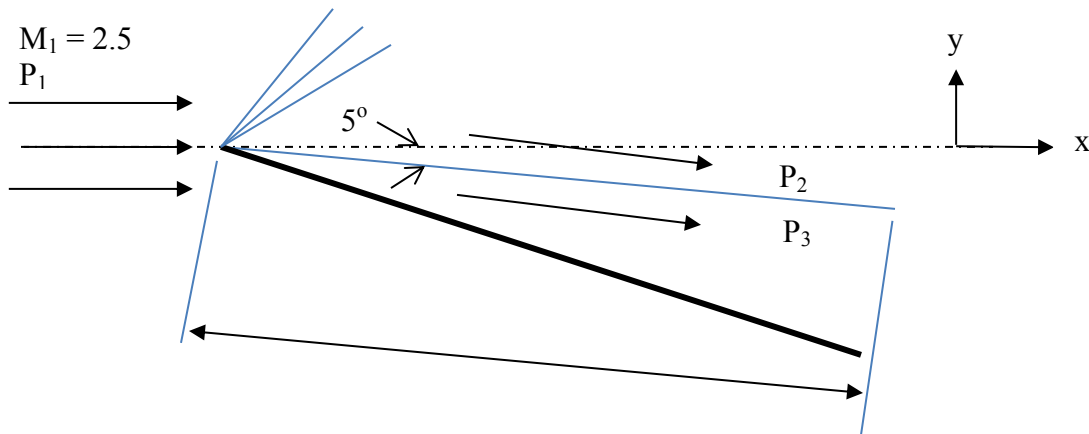

Figure 3.30. Geometry for Example 3.3 (side-view)

Solution:
  a. In the lower surface, an oblique shock is formed. The pressure P3 is determined as follows:

$$\tan\theta = 2\cot\beta\left[\frac{M_1^2\sin^2\beta - 1}{M_1^2(\gamma + \cos 2\beta) + 2}\right] \Rightarrow \tan(5) = 2\cot\beta\left[\frac{2.5^2\sin^2\beta - 1}{2^2(1.4 + \cos 2\beta) + 2}\right] \qquad (3.44)$$

The solution of this nonlinear equation yields an angle of 27.4 degrees (β = 27.4 deg). The normal component to the shock M_{n1} is:

$$M_{n1} = M_1\sin\beta = 2\sin(27.4) = 1.15 \qquad (3.43)$$

The static pressure behind the oblique shock wave is:

$$P_3 = P_1\left[1 + \frac{2\gamma}{\gamma + 1}(M_{n1}^2 - 1)\right] = 101,325\left[1 + \frac{2(1.4)}{1.4 + 1}(1.15^2 - 1)\right] \qquad (3.42)$$

$$\Rightarrow P_3 = 139,823 \quad Pa$$

b. In the upper surface, an oblique shock is formed. The pressure P_2 is determined as follows:

For forward Mach line:

$$v_1(M) = \sqrt{\frac{\gamma + 1}{\gamma - 1}}\tan^{-1}\left[\sqrt{\frac{\gamma - 1}{\gamma + 1}(M_1^2 - 1)}\right] - \tan^{-1}\left[\sqrt{(M_1^2 - 1)}\right] \qquad (3.51)$$

$$v_1(M) = \sqrt{\frac{1.4 + 1}{1.4 - 1}}\tan^{-1}\left[\sqrt{\frac{1.4 - 1}{1.4 + 1}(2.5^2 - 1)}\right] - \tan^{-1}\left[\sqrt{(2.5^2 - 1)}\right] = 39.1 \quad deg \qquad (3.51)$$

$$\theta = v(M_2) - v(M_1) \Rightarrow v(M_2) = v(M_1) + \theta = 39.1 + 5 = 44.12 \quad deg \qquad (3.50)$$

For rearward Mach line:

$$v_2(M) = \sqrt{\frac{\gamma + 1}{\gamma - 1}}\tan^{-1}\left[\sqrt{\frac{\gamma - 1}{\gamma + 1}(M_2^2 - 1)}\right] - \tan^{-1}\left[\sqrt{(M_2^2 - 1)}\right] \qquad (3.51)$$

$$44.12 = \sqrt{\frac{1.4 + 1}{1.4 - 1}}\tan^{-1}\left[\sqrt{\frac{1.4 - 1}{1.4 + 1}(M_2^2 - 1)}\right] - \tan^{-1}\left[\sqrt{(M_2^2 - 1)}\right] \qquad (3.51)$$

Solution of this nonlinear equation yields:

$$M_2 = 2.723 \qquad (3.51)$$

The static pressure behind the expansion wave is:

$$P_2 = P_1\left[\frac{1 + \frac{\gamma - 1}{2}M_1^2}{1 + \frac{\gamma - 1}{2}M_2^2}\right]^{\frac{\gamma}{\gamma - 1}} = 101325\left[\frac{1 + \frac{1.4 - 1}{2}(2.5)^2}{1 + \frac{1.4 - 1}{2}(2.723)^2}\right]^{\frac{1.4}{1.4 - 1}} = 71,742 \quad Pa \qquad (3.49)$$

c. Drag

The wave drag force is the x-component of the pressure force:

$$D_w = (P_3 - P_2)bC\sin\alpha = (139{,}823 - 71{,}512)\times 5\times 2\times \sin(5) = 59{,}336 \ N \tag{3.41}$$

The wave drag coefficient is:

$$C_{D_w} = \frac{D_w}{\dfrac{1}{2}\gamma\cdot M_1^2 P_1 S} = \frac{59{,}336}{0.5\times 1.4\times 2.5^2 \times 101{,}325\times 5\times 2} \tag{3.40}$$

$$\Rightarrow C_{D_w} = 0.0134$$

3.5.2. Aircraft Wave Drag

An aircraft has usually a complex geometry and various components. In previous section, mathematical technique was introduced to calculate the wave drag where the object has a very simple (e.g., flat plate, wedge) configuration. Every aircraft component contributes to wave drag. In this section, a technique is presented to determine the wave drag of a complete aircraft.

In this approach, we consider an aircraft as a whole and we will not divide it into several components. This is an approximate and empirical technique [8]. The aircraft wave drag coefficient consists of two parts; volume-dependent wave drag (C_{Dwv}), and lift-dependent wave drag (C_{Dwl}). The volume-dependent wave drag is a function of aircraft volume and much greater than lift-dependent wave drag. The reason is that, at supersonic speeds, the lift coefficient (C_L) is very minimal.

$$C_{D_w} = C_{D_{wl}} + C_{D_{wv}} \tag{3.52}$$

The lift-dependent wave drag is given by:

$$C_{D_{wl}} = \frac{K_{wl}SC_L^2(M^2-1)}{2\pi L^2} \tag{3.53}$$

where L represents the aircraft fuselage length, S is wing reference area, and K_{wl} is a parameter given by

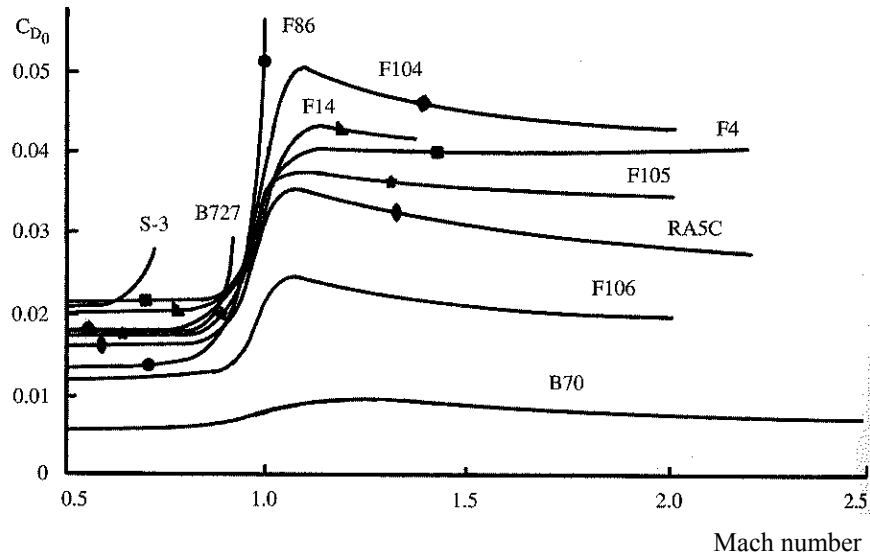$$K_{wl} = 2\left(\frac{S}{bL}\right)^2 \tag{3.54}$$

and b is the wing span.

Figure 3.31. *Wave drag for several aircraft (Ref. 9)*

The volume-dependent wave drag is given by:

$$C_{D_{wv}} = \frac{128 K_{wv} V^2}{\pi S L^4}$$

(3.55)

where V is the total aircraft volume and K_{wv} is a factor given by:

$$K_{wv} = 1.17 \left(\frac{1 + 0.75\beta \dfrac{b}{L}}{1 + 2\beta \dfrac{b}{L}} \right)$$

(3.56)

and β is a function of Mach number as

$$\beta = \sqrt{M^2 - 1}$$

(3.57)

In general, wave drag is significant, such that it will increase the aircraft drag up to about two to three times compared with subsonic drag. For instance, C_{Do} of fighter aircraft F-4 at Mach number 1.5 (supersonic) is about 0.045, while its C_{Do} at Mach number 0.6 (subsonic) is about 0.016. Figure 3.31 shows zero-lift drag coefficients of several aircraft for a range of Mach numbers from subsonic to supersonic speeds. The drag rise of most of the aircraft due to high Mach number is considerably high. Table 3.8 illustrates C_{Do} of several aircraft at their cruise speed.

3.6. C_{Do} for Various Configurations

Any individual aircraft will often take various configurations in flight phases. When an aircraft retracts its landing gear, deflects its flap, rotates its control surfaces, exposes any external component (such as gun), releases its store (e.g., missile), or opens its cargo door; it has changed its configuration. In general, there are three configuration groups

that an aircraft may adopt, they are: 1. clean configuration, 2. take-off configuration, and 3. landing configuration.

The clean configuration is the aircraft configuration employed at flight phases such as cruise, climb and turn. As the names imply, the take-off configuration, and landing configuration are the aircraft configurations which are adopted during take-off and landing respectively. In an aircraft with a retractable landing gear, the landing gear are employed during take-off and landing and retracted during cruising flight. Furthermore, the flaps are extended in take-off and landing operations. The flap deflection angle is a function of aircraft payload weight and atmospheric conditions.

No	Aircraft	Engine	No. of Engines	Landing gear	C_{Do}
1	Pilatus PC-9	Turboprop	1	Retractable	0.022
2	Lockheed F-104 Starfighter	Turbojet	1	Retractable	0.016
3	Embraer EMB 312 Tucano	Turboprop	1	Retractable	0.021
4	Boeing 747	Turbofan	4	Retractable	0.018
5	Lockheed Jetstar	Turbojet	4	Retractable	0.0185
6	Lockheed C-5 Galaxy	Turbofan	4	Retractable	0.019
7	Boeing 727	Turbofan	3	Retractable	0.07
8	Grumman F-14 Tomcat	Turbofan	2	Retractable	0.02
9	Learjet 25	Turbofan	2	Retractable	0.022
10	Douglas C-54 Skymaster	Piston prop	4	Retractable	0.023
11	Curtiss C-46 Commando	Turboprop	2	Retractable	0.025
12	Beech V35 Bonanza	Turboprop	1	Retractable	0.025
13	Cessna 310	Piston prop	2	Retractable	0.025
14	McDonnell Douglas F-4 Phantom	Turbojet	2	Retractable	0.03
15	Piper PA-28	Piston prop	1	Fixed	0.047
16	Cessna 172	Piston prop	1	Fixed	0.028
17	North American F-86 Sabre	Turbojet	1	Retractable	0.014
18	North American XB-70 Valkyrie	Turbojet	6	Retractable	0.006
19	F-106 Convair Delta Dart	Turbojet	1	Retractable	0.013
20	McDonnell Douglas (now Boeing) F/A-18 Hornet	Turbofan	2	Retractable	0.017

Table 3.8. C_{Do} of several aircraft

3.6.1. Clean Configuration

The clean configuration is the configuration of an aircraft when it is at a cruise flight condition. At this configuration, no flap is deflected, and landing gear is retracted (if it is retractable). Therefore the drag polar is

$$C_{D_{clean}} = C_{D_{o_{clean}}} + K\left(C_{L_C}\right)^2 \tag{3.58}$$

Thus, clean C_{Do} of the aircraft ($C_{D_{o_{clean}}}$) includes every component (such as wing, tail, and fuselage), and excludes flap and landing gear (if retractable). If the landing gear is not

retractable (e.g., as in Cessna 172), the C_{Do} includes landing gear too. The parameter C_{LC} is the cruise lift coefficient.

3.6.2. Take-Off Configuration

The take-off configuration is the configuration of an aircraft when it is at take-off condition. In this configuration, the aircraft has high angle of attack, flap is deflected for take-off, and landing gear is not retracted (even if it is retractable). In a take-off condition, the flaps are usually deflected down about 10-30 degrees. The take-off C_{Do} depends on type and the deflection angle of the flaps. As the flap deflection increases, the take-off C_{Do} increases too. The drag polar at take-off configuration is

$$C_{D_{TO}} = C_{D_{oTO}} + K\left(C_{L_{TO}}\right)^2 \qquad (3.59)$$

where, the take-off zero-lift drag coefficient is given by

$$C_{D_{oTO}} = C_{D_{oclean}} + C_{D_{oflap-TO}} + C_{D_{oLG}} \qquad (3.60)$$

where $C_{D_{oflap-TO}}$ represents the zero-lift drag coefficient of flap at take-off condition. In addition, the parameter $C_{D_{oLG}}$ represents the zero-lift drag coefficient of the landing gear. Moreover, C_{LTO} represents the lift coefficient at take-off. This coefficient does not have a constant value during take-off, due to the accelerated nature of the motion. The C_{LTO} at the lift-off condition (where the front wheel is just detached from the ground), is given by

$$C_{L_{TO}} \cong 0.9 \frac{2mg}{\rho S(V_{LO})^2} \qquad (3.61)$$

where V_{LO} represents the aircraft lift-off speed. The factor of 0.9 is added due to the contribution of the engine thrust during take-off in vertical direction. The aircraft lift-off speed is often about 10%-30% higher than the aircraft stall speed.

$$V_{LO} = K_{LO}V_S \qquad (3.62)$$

where $K_{LO} = 0.1 - 0.3$. In Chapter 8, the take-off performance will be discussed in great details.

3.6.3. Landing Configuration

The landing configuration is the configuration of an aircraft when it is at landing condition. In this configuration, the aircraft has high angle of attack (even more than take-off condition), flap is deflected (even more than take-off condition), and landing gear is not retracted (even if it is retractable). In landing condition, the flaps are usually deflected down about 30-60 degrees. The landing C_{Do} depends of the deflection angle of the flaps. As this angle increases, the landing C_{Do} increases too. The landing zero-lift drag coefficient (C_{DoL}) is often greater than the take-off zero-lift drag coefficient (C_{DoTO}). If there is another means of high lift device for the aircraft, such as slat, you need to add it to this equation. The drag polar at landing configuration is given by:

$$C_{D_L} = C_{D_{oL}} + K\left(C_{L_L}\right)^2 \qquad (3.63)$$

where C_{L_L} is the lift coefficient at landing and is given by:

$$C_{L_L} \cong \frac{2mg}{\rho S (V_L)^2} \tag{3.64}$$

where V_L is the aircraft landing speed. The landing speed (V_L) and is often about 10%-30% greater than the stall speed.

$$V_L = K_L V_S \tag{3.65}$$

where $K_L = 0.1 - 0.3$. The landing zero-lift drag coefficient is given by

$$C_{D_{oL}} = C_{D_{oclean}} + C_{D_{oflap-L}} + C_{D_{oLG}} \tag{3.66}$$

where $C_{D_{oflap-L}}$ represents the zero-lift drag coefficient of the flap at landing condition. Both $C_{D_{oflap-TO}}$ and $C_{D_{oflap-L}}$ are functions of flap deflection. In Chapter 8, the landing performance will be presented.
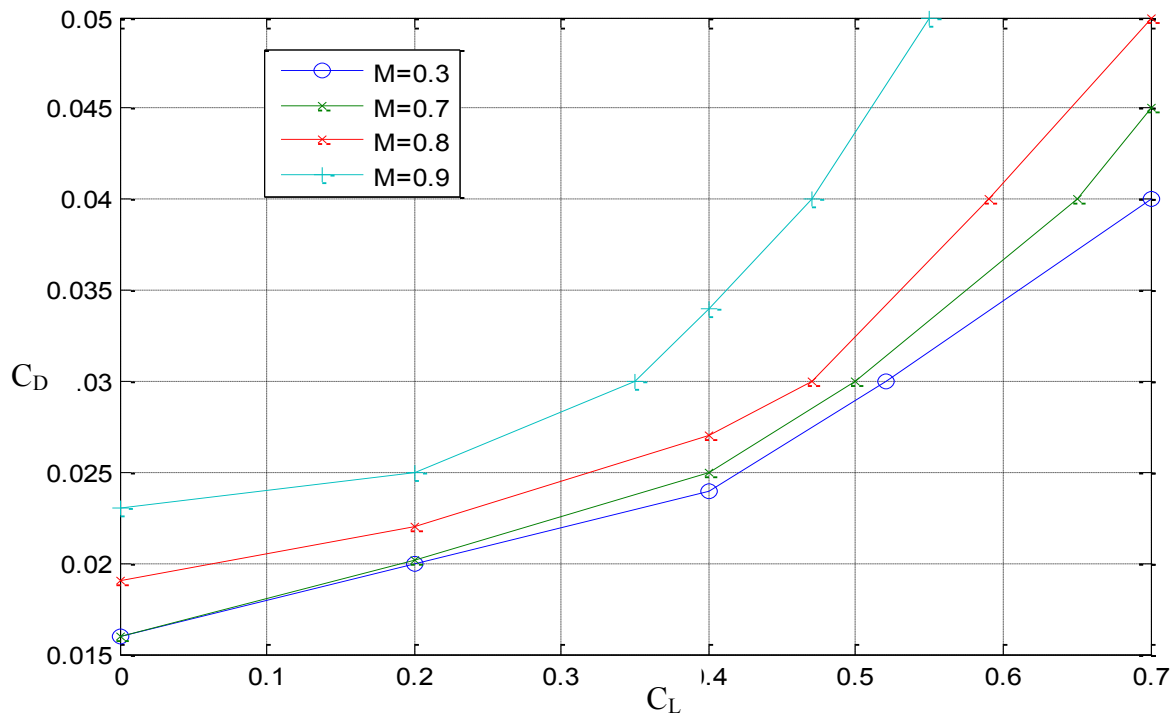

Figure 3.32. *Drag coefficient versus lift coefficient for various Mach number*

3.6.4. The Effect of Speed and Altitude on C_{Do}

The aircraft zero-lift drag coefficient is a function of a number of flight parameters. Reynolds number is one of the influential parameters on the zero-lift drag coefficient. As the Reynolds number increases, the boundary layer thickness decreases and thus C_{Do} decreases as well. As equation 3.16 indicates, the Reynolds number is a function of true airspeed. Since the true airspeed is a function of altitude (indeed, air density), it can be concluded that the Reynolds number is also a function of altitude. Another factor

affecting C_{D_o} is the compressibility which is significant at speeds higher than Mach 0.7. The third important factor is the wave drag as discussed in section 3.5. Considering these factors, it is concluded that the C_{D_o} is a function of Mach number and altitude:

$$C_{D_o} = f(M, h) \tag{3.67}$$

At low subsonic Mach numbers, C_{D_o} is increased, due to an increase in Reynolds number. As compressibility factor shows up in higher subsonic speeds, the C_{D_o} increases with a higher rates. In transonic speeds, shock wave is formed and a jump (sudden increase) in C_{D_o} will be experienced. Therefore, the C_{D_o} is directly proportional with speed, and as speed (Mach number) is increased, the C_{D_o} increases. Figure 3.32 illustrates typical variations of drag coefficient versus lift coefficient at various subsonic Mach numbers.

The second factor that affects the C_{D_o} is altitude. For a specific Mach number, as the altitude increases, the true airspeed decreases. For instance, consider an aircraft is flying with a speed of Mach 0.5 at sea level. The true airspeed at this altitude is 170 m/sec (0.5 × 340 = 170). If this aircraft is flying with the same Mach number at 11,000 ft altitude, the true airspeed will be 147 m/sec (0.5 × 249 = 147). In addition, the air density decreases with altitude with a higher rate. Thus, the higher altitude means the lower Reynolds number (Equation 3.22), and therefore the higher C_{D_o}. Figure 3.33 illustrates the variations of drag force for a light transport aircraft with turbofan engines at various altitudes. This transport aircraft has a stall speed of 90 knots and a maximum speed of 590 knots.
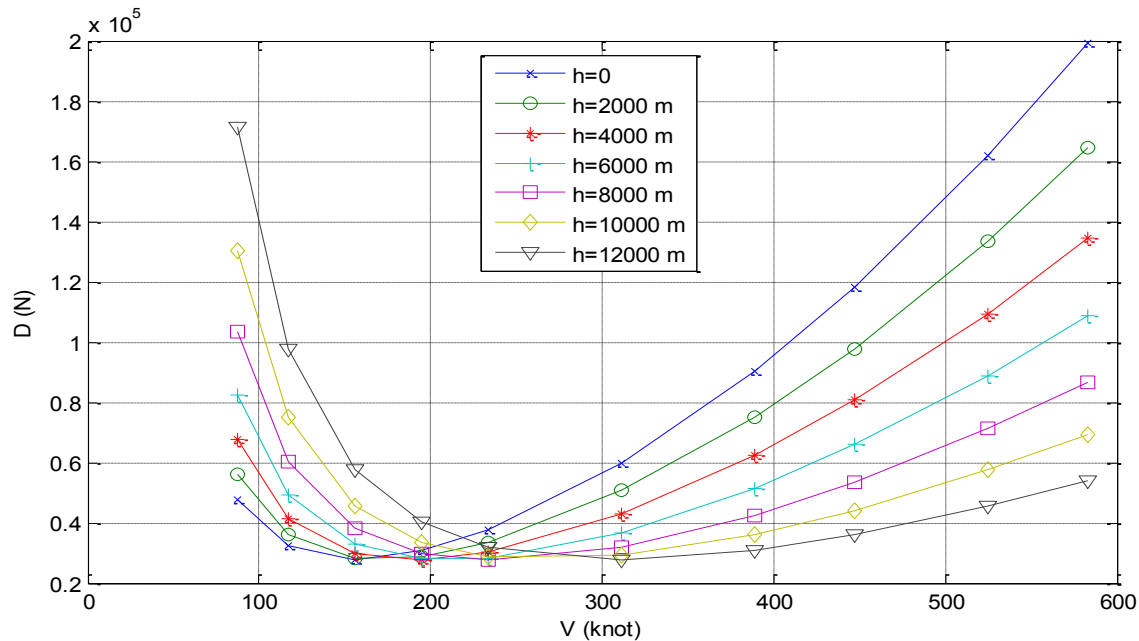

Figure 3.33. *Variations of drag force without considering the compressibility effects*

In conclusion, it can be assumed that at the Mach numbers less than 0.7, the variation of C_{Do} is not significant such that it can be considered constant. At higher Mach numbers, the compressibility effect and wave drag must be taken into account. The second conclusion is that, at higher altitude, total drag force is reduced. The reason is that, although at higher altitude, the C_{Do} is increased, but the air density decreases. The rate of change (decrease) in air density is faster than the rate of change (increase) of C_{Do}. This is one of the reasons why airlines choose to fly at higher altitudes despite the need and cost of climb.

Example 3.4

Consider the aircraft in example 3.1 is equipped with a single-slotted flap with an average flap chord of 2.3 m. The aircraft takes off with a flap angle of 20 degrees and lands with a flap angle of 35 degrees. Assume the C_{Do} of landing gear is 0.01, induced drag correction factor; K is 0.052; and both take-off and landing speeds are 130 knot. Determine the aircraft C_{Do} at take-off and landing configurations.

Solution:

The C_{Do} of the flap is given by

$$C_{D_{o\,flap}} = \left(\frac{C_f}{C}\right) A \cdot \left(\delta_f\right)^B \tag{3.26}$$

From Table 3.3, A = 0.00018 and B = 2, so

The C_{Do} of flap at take-off is

$$C_{D_{o\,flap}} = \left(\frac{2.3}{9.3}\right) \times 0.00018 \times (20)^2 = 0.0178 \tag{3.26}$$

The C_{Do} of the flap at landing is

$$C_{D_{o\,flap}} = \left(\frac{2.3}{9.3}\right) \times 0.00018 \times (35)^2 = 0.0545 \tag{3.26}$$

The take-off C_{Do}:

$$C_{D_{oTO}} = C_{D_{oclean}} + C_{D_{oflap-TO}} + C_{D_{oLG}} = 0.023 + 0.0178 + 0.01 = 0.051 \tag{3.47}$$

To find aircraft drag coefficient, we need to determine the induced drag coefficient. The lift coefficient at take-off is:

$$C_{L_{TO}} \cong 0.9 \frac{2mg}{\rho S (V_{LO})^2} = \frac{0.9 \times 2 \times 380000 \times 9.81}{1.225 \times 567 \times (130 \times 0.5144)^2} = 2.16 \tag{3.49}$$

$$C_{D_i} = K C_L^2 = 0.052 \times 2.16^2 = 0.242 \tag{3.12}$$

So, C_{DTO} is

$$C_{D_{TO}} = C_{D_{o_{TO}}} + K\left(C_{L_{TO}}\right)^2 = 0.051 + 0.243 = 0.293 \tag{3.48}$$

For the landing:

$$C_{L_L} \cong \frac{2mg}{\rho S \left(V_{LO}\right)^2} = \frac{2 \times 380000 \times 9.81}{1.225 \times 567 \times \left(130 \times 0.5144\right)^2} = 2.4 \tag{3.52}$$

$$C_{D_i} = K \cdot C_L^{\ 2} = 0.052 \times 2.4^2 = 0.3 \tag{3.12}$$

$$C_{D_{oL}} = C_{D_{o_{clean}}} + C_{D_{o_{flap-L}}} + C_{D_{o_{LG}}} = 0.023 + 0.0545 + 0.01 = 0.088 \tag{3.47}$$

$$C_{D_L} = C_{D_{oL}} + K\left(C_{L_L}\right)^2 = 0.088 + 0.3 = 0.387 \tag{3.48}$$

Problems

Note: In all problems, assume ISA condition, unless otherwise stated.

1. A GA aircraft is flying at 5,000 ft altitude. The length of the fuselage is 7 m, wing mean aerodynamic chord is 1.5 m, horizontal tail mean aerodynamic chord is 1.5 m, and vertical tail mean aerodynamic chord is 0.6 m. Determine Reynolds number of fuselage, wing, horizontal tail and vertical tail.

2. The following (figure 3.34) is a top-view of Boeing 757 transport aircraft that has a wing span of 38.05 m. Using a proper scale and using a series of measurements, determine the wing reference (gross) area, and wing net area of this aircraft.
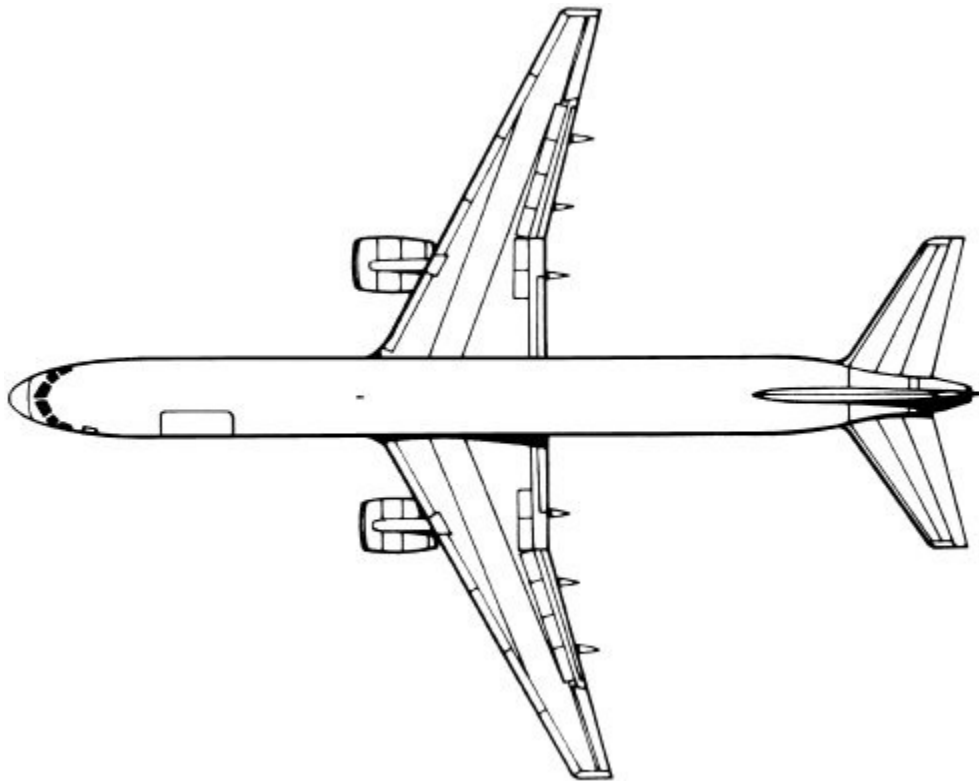

Figure 3.34. *Top-view of Boeing 757 transport aircraft*

3. Estimate the wing wetted area of Boeing 757 (problem 2). Assume the wing has a maximum thickness of 12%.

4. The mean aerodynamic chord of a trainer aircraft is 3.1 m. This trainer is cruising at sea level with a speed of Mach 0.3. Determine skin friction coefficient of the wing when boundary layer over the wing is: a. laminar, b. turbulent.

5. A business jet aircraft with a 31 m^2 wing area and a mass of 6,500 kg is flying at 10,000 ft altitude with a speed of 274 knot. If $C_{Do} = 0.026$, $K = 0.052$, $C_{Lmax} = 1.8$, calculate and plot the following items:

a. drag polar
b. variation of drag force with speed.

6. The tip chord of a wing is 6 m and its root chord is 9 m. What is the mean aerodynamic chord?

7. The Attack aircraft Thunderbolt II (Fairchild A-10) has the following features: m_{TO} = 22,221 kg, S = 47 m^2, K = 0.06, C_{Do} = 0.032, V_{max} = 377 knot, V_{TO} = 120 knot. Assume that the C_{Do} is constant throughout all speeds.

    a. Plot the Variation of zero-lift drag (D_o) versus speed (from take-off speed to maximum speed)
    b. Plot the Variation of induced drag (D_i) versus speed (from take-off speed to maximum speed)
    c. Plot the Variation of total drag (D) versus speed (from take-off speed to maximum speed)
    d. At what speed, the drag force is minimum?

8. The wing of the twin-turbofan airliner Boeing 777 has a 31.6 degrees of leading edge sweepback, a span of 60.93 m and a planform area of 427.8 m^2. Determine Oswald efficiency factor (e) and induced drag correction factor (K) for this wing.

9. Determine the Oswald efficiency factor of a rectangular wing with an aspect ratio of 14.

10. A single engine trainer aircraft with a wing area of 26 m^2 has a fixed landing gear with three similar tires. Each tire has a diameter of 25 cm and a thickness of 7 cm. Each tire is connected to the fuselage with a strut with a diameter of 4 cm and a length of 15 cm. The landing gear does not have fairing, determine zero-lift drag coefficient of the landing gear.

11. A cargo airplane is cruising with a speed of Mach 0.47, is taking off with a speed of 95 knot and is landing with a speed of 88 knot. The plain flap with a 20% chord ratio is deflected down 22 degrees during take-off and 35 degrees during landing. The aircraft has a mass of 13,150 kg, a wing area of 41.2 m^2, and induced drag correction factor, K is 0.048. The zero lift drag coefficients of all components are
    C_{Dow} = 0.008, C_{Dof} = 0.006, C_{Doht} = 0.0016, C_{Dovt} = 0.0012, C_{Don} = 0.002, C_{DoLG} = 0.015, C_{Dos} = 0.004,
    Determine drag force at
a. cruise
b. take-off
c. landing

12. A Swedish aircraft designer is designing a fuselage for a 36-passenger aircraft to cruise at a Mach number of 0.55. He is thinking of two seating arrangement

options: a. 12 rows of three passengers, and b. 18 rows of two passengers. If he selects option a, the fuselage length would be 19.7 m with a diameter of 2.3 m. In option b the fuselage length would be 27.2 m with a diameter of 1.55 m. What option yields the lowest fuselage zero-lift drag coefficient?

13. The amphibian airplane Lake LA-250 (figure 3.35) has a wing with the following features:
$S = 15.24$ m^2, b = 11.68 m, MAC =1.35 m, $(t/c)_{max}$ = 15%, airfoil: NACA 4415, $C_{dminw} = 0.0042$
The aircraft has a mass of 1,678 kg and is cruising with a speed of 155 knot. Determine the wing zero-lift drag coefficient. For other information, use the aircraft three-view that is provided.
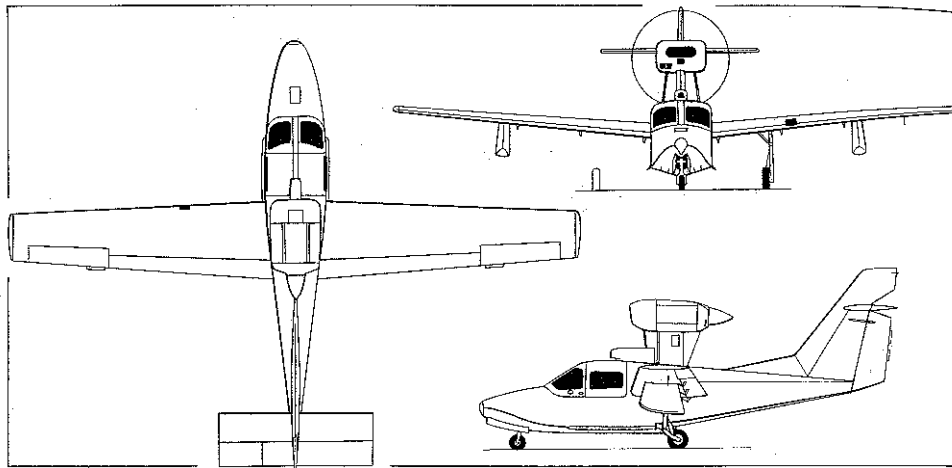

Figure 3.35. *Three-view of amphibian airplane Lake LA-250*

14. Assume that the aircraft in problem 13 has a plain flap with a chord ratio of 0.2. Determine the flap C_{Do}, when it is deflected 30 degrees during a take-off operation.

15. A twelve-seat commuter airplane has a vertical tail with the following features: S_{vt} = 4.3 m^2, b_{vt} = 5.4 m, $(t/c)_{max\_vt}$ = 10%, C_{dmin_vt} = 0.005. The aircraft has a wing area of 29.4 m^2 and is cruising with a true airspeed of 160 knot at an altitude of 18,000 ft ISA condition. Determine the vertical tail zero-lift drag coefficient.

16. The four-seat light airplane Piper PA-34 has a horizontal tail with the following features:
S_{ht} = 3.6 m^2, b_{ht} = 4.14 m, $(t/c)_{max\_ht}$ = 12%, $C_{dmin-ht}$ = 0.0047
 The aircraft has a mass of 2,154 kg, a wing area of 19.39 m^2 and is cruising at 171 knot at an altitude of 18,500 ft. Determine the horizontal tail zero-lift drag coefficient.

17. A jet trainer with a retractable landing gear has the following features:

m_{TO} = 5,630 kg, S = 25.1 m^2, b = 17.4 m, e = 0.85, V_c = 270 knot, C_{Lmax} = 2.2, V_{TO} = 1.2 V_s, V_{Land} = 1.3 V_s, $C_{Doclean}$ = 0.032, $C_{DoflapTO}$ = 0.02, $C_{DoflapLand}$ = 0.035, C_{DoLG} = 0.01.

Determine the aircraft drag at three flight conditions: a. clean (cruise speed) , take-off, and c. landing.

18. The wings of the Y-5B agricultural biplane are connected together thru two struts. Each strut has a circular cross section with the length of 1.2 m and a diameter of 4 cm. The total planform area of both wings is 38 m^2; determine the zero-lift drag coefficient of struts.

19. A single-engine small aircraft has a wing area of 26 m^2 and a turboprop engine that has a power of 600 hp. The aircraft is cruising at 25,000 ft altitude with a speed of 182 knot. Determine the engine cooling drag coefficient. Assume K_e = 2.

20. A business jet aircraft with a wing area of 45 m^2 is equipped with two turbofan engines. Each engine is podded in a nacelle with a diameter of 62 cm and a length of 110 cm. Determine nacelle zero-lift drag coefficient, provided the aircraft is cruising with a speed of 320 knot at an altitude of 28,000 ft.

21. A maneuverable aircraft has two fuel tanks at the wingtips. Each fuel tank has a shape of an ellipsoid with a diameter of 20 cm and a length of 130 cm. Determine fuel tank zero-lift drag coefficient, provided the aircraft is cruising with a speed of 190 knot at an altitude of 18,000 ft.

22. The F-16 supersonic jet fighter (figure 3.36) with a mass 12,331 kg and a wing area of 27.8 m^2 is cruising at an altitude of 40,000 ft at Mach number 2.1. The wing span is 9.45 m and length of the fuselage is 15.3 m. Determine wave drag of the aircraft, assuming the aircraft volume is 21.3 m^2.

23. Assume that F-16 (problem 22) is flying at a Mach number of 1.2 at the same altitude. What is wave drag of this fighter at this flight condition? Compare the result with the result of problem 22 and comment about your finding.
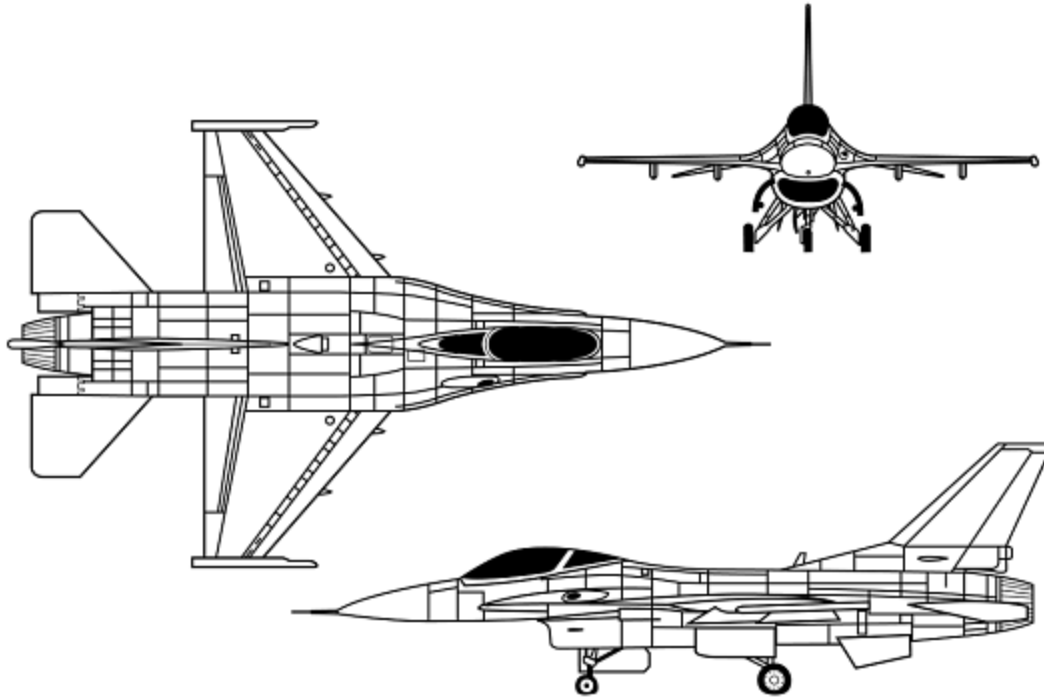
Figure 3.36. *The three-view of Fighter jet F-16A*

24. The fuselage of a large transport aircraft has a diameter of 3.8 m and a length of 43 m. Determine the fuselage zero-lift drag, assuming the wing area to be 180 m^2 and cruising speed to be 350 knot at 35,000 ft.

25. Determine the terminal velocity of a water droplet; assuming it has a shape of a sphere with a radius of 2 mm. The density of water is 998 kg/m^3.

26. You are required to design a parachute for the safe landing of a paratrooper with a mass of 85 kg. Determine the diameter of the parachute, if the terminal velocity is required to be 1 m/s at 5000 ft altitude. Ignore the drag of the paratrooper and strings. The mass of the parachute is 6 kg.

27. Felix Baumgartner, an Austrian daredevil fell to Earth from more than 24 miles high, becoming the first human to break the sound barrier under his own power, on October 14, 2012. He made the highest and fastest jump in history after ascending by a helium balloon to an altitude of 128,100 feet, reaching a maximum speed of Mach 1.24. Assume the terminal velocity was at 70,000 ft, and his frontal area while descending is 0.12 m^2; determine drag coefficient of his body.

28. Consider a very thin flat plate wing with a chord of 0.4 m and a span of 3.6 m. The wing is placed at a 6° angle of attack in a Mach 1.3 air flow. Determine the wave drag coefficient.

29. Consider a 2% thickness flat plate wing with a chord of 1.2 m and a span of 4.5 m. The wing is placed at a 3° angle of attack in a Mach 1.7 air flow. Determine

a. wing zero-lift drag coefficient
b. induced drag coefficient
c. wing wave drag coefficient.

Assuming the aircraft has a mass of 1000 kg and is cruising at an altitude of 12,000 ft. The wing Cd_{min} may be assumed to be 0.003, and Oswald efficiency factor to be 0.8.

30. Consider a rectangular wing with a span of 15 m and a chord of 3 m in a Mach 2.6 air flow (the side-view as sketched in figure 3.28). The airfoil section is a 7° half-angle wedge at zero angle of attack. Calculate the wave drag coefficient. Assume that the expansion over the corners of the base is such that, the base pressure is equal to the free-stream pressure.

31. Consider a tapered wing with a span of 12 m and a chord of 2.5 m in a Mach 1.5 air flow (the side-view as sketched in figure 3.28). The airfoil section is a 4° half-angle wedge at zero angle of attack. Calculate the wave drag coefficient. Assume that the expansion over the corners of the base is such that, the base pressure is equal to the free-stream pressure. The wing taper ratio is 0.4.

References

1. Hoak D. E., USAF Stability and Control Datcom, Air Force Flight Dynamics Laboratory, Wright-Patterson Air Force Base, Ohio, 1978
2. McCormick B. W., Aerodynamics; Aeronautics; and Flight Dynamics, John Wiley, 1995
3. Abbott I. H., and von Doenhoff A. E., Theory of Wing Sections, Dover, 1959
4. Horner S. R., Fluid-Dynamic Drag, Midland Park, NJ, 1965
5. Ross R., Neal R.D., Learjet Model 25 Drag Analysis, Proceeding of the NASA-Industry-University GA drag reduction workshop, Lawrence, KS, July 14-16, 1975
6. Shevell R., Fundamentals of Flight, Second Edition, Prentice Hall, 1989
7. Anderson J., Modern Compressible Flow, Third edition, McGraw-Hill, 2005
8. Kuchemann D., Aerodynamic Design of Aircraft, Pergamon Press, 1978
9. Raymer D. P, Aircraft Design: A Conceptual Approach, AIAA, 2006
10. Anderson J., Fundamentals of Aerodynamics, third edition, McGraw-Hill, 2005
11. Roskam J., Airplane Design, Volume VI, DAR Corp., 2004
12. Paul Jackson, et al., Jane's all the World's Aircraft, Jane's Information Group, several years
13. Cengel Y. A., and Cimbala J. M., Fluid Mechanics: Fundamentals and Applications, 3rd edition, McGraw-Hill, 2013.
14. Stinton D., The Anatomy of the Airplane, Second Edition, AIAA, 1998
15. Lan E. C. and Roskam J., Airplane Aerodynamics and Performance, DAR Corp., 2003
16. www.airliners.net